Landsc Ecol (2025) 40:37
https://doi.org/10.1007/s10980-025-02054-8

RESEARCH ARTICLE

Microclimate temperature effects propagate across scales in forest ecosystems

Kristin H. Braziunas · Werner Rammer · Pieter De Frenne · Joan Díaz-Calafat · Per-Ola Hedwall · Cornelius Senf · Dominik Thom · Florian Zellweger · Rupert Seidl

Received: 23 July 2024 / Accepted: 24 January 2025

Abstract
Context Forest canopies shape subcanopy environments, affecting biodiversity and ecosystem processes. Empirical forest microclimate studies are often restricted to local scales and short-term effects, but forest dynamics unfold at landscape scales and over long time periods.
Objectives We developed the first explicit and dynamic implementation of microclimate temperature buffering in a forest landscape model and investigated effects on simulated forest dynamics and outcomes.
Methods We adapted the individual-based forest landscape and disturbance model iLand to use microclimate temperature for three processes [decomposition, bark beetle (*Ips typographus* L.) development, and tree seedling establishment]. We simulated forest dynamics with or without microclimate temperature buffering in a temperate European mountain landscape under historical climate and disturbance conditions.
Results Temperature buffering effects propagated from local to landscape scales. After 1,000

Supplementary Information The online version contains supplementary material available at https://doi.org/10.1007/s10980-025-02054-8.

K. H. Braziunas (✉) · W. Rammer · D. Thom · R. Seidl
Ecosystem Dynamics and Forest Management Group, School of Life Sciences, Technical University of Munich, 85354 Freising, Germany
e-mail: kbraziun@uw.edu

Present Address:
K. H. Braziunas
School of Environmental and Forest Sciences, University of Washington, Seattle, WA 98195, USA

P. De Frenne
Forest & Nature Lab, Department of Environment, Faculty of Bioscience Engineering, Ghent University, 9090 Melle-Gontrode, Belgium

J. Díaz-Calafat · P.-O. Hedwall
Southern Swedish Forest Research Centre, Swedish University of Agricultural Sciences, 234 56 Alnarp, Sweden

C. Senf
Earth Observation for Ecosystem Management, School of Life Sciences, Technical University of Munich, 85354 Freising, Germany

D. Thom
Chair of Silviculture, Institute of Silviculture and Forest Protection, TUD Dresden University of Technology, 01737 Tharandt, Germany

F. Zellweger
Swiss Federal Research Institute WSL, 8903 Birmensdorf, Switzerland

R. Seidl
Berchtesgaden National Park, 83471 Berchtesgaden, Germany

Published online: 03 February 2025

simulation years, average total carbon and cumulative net ecosystem productivity were 2% and 21% higher, respectively, and tree species composition differed in simulations including versus excluding microclimate buffering. When microclimate buffering was included, Norway spruce (*Picea abies* (L.) Karst.) increased by 9% and European beech (*Fagus sylvatica* L.) decreased by 12% in mean basal area share. Some effects were amplified across scales, such as a mean 16% decrease in local-scale bark beetle development rates resulting in a mean 45% decrease in landscape-scale bark beetle-caused mortality.

Conclusions Microclimate effects on forests scaled nonlinearly from stand to landscape and days to millennia, underlining the utility of complex simulation models for dynamic upscaling in space and time. Microclimate temperature buffering can alter forest dynamics at landscape scales.

Keywords Climate regulation · Forest landscape model development · Microclimate · European Alps · Process-based models · Temperate mountain forests

Introduction

Forest canopies shape local environments, creating microclimatic conditions that affect ecosystem structure and processes (Geiger 1950). For example, forests modify subcanopy radiation, air and soil temperature, precipitation, wind, relative humidity, soil moisture, and snowpack duration and distribution (Chen et al. 1999; Storck et al. 2002). Near-surface climate affects a wide range of forest processes and services, including tree seedling establishment, understory species composition and cover, wildlife habitat and metabolism, decomposition rates, and disturbance intensity and effects (Chen et al. 1999; Hoecker et al. 2020; Zellweger et al. 2020; De Frenne et al. 2021; Reiner et al. 2021).

A key characteristic of forest microclimates is that temperature extremes are reduced below canopies compared to free-air conditions outside forests, leading to a microclimate buffering effect (De Frenne et al. 2021). Temperature buffering is well documented globally across multiple forest types, on average cooling maximum air temperatures by 2.7°C and warming minimum air temperatures by 1.2°C in temperate forests (De Frenne et al. 2019). Among other factors, microclimate buffering is shaped by topography and canopy structure and composition via their effects on local radiation regimes, evapotranspiration levels, and air mixing (Chen et al. 1999; De Frenne et al. 2021). Microclimate buffering by forests is expected to become increasingly important given ongoing global climate warming because of its sensitivity to macroclimate (i.e., free-air climate in open areas) temperature, with greater canopy-mediated cooling at higher maximum temperatures (De Frenne et al. 2019; Thom et al. 2020; De Lombaerde et al. 2022). As a result, microclimate warming may lag behind macroclimate warming, with implications for future forest biodiversity, species microrefugia and distributional range shifts, and carbon mitigation potential (Lenoir et al. 2017; Zellweger et al. 2020; Pastore et al. 2022; Sanczuk et al. 2023).

Forest dynamics play out at landscape scales (i.e., 10^3 to 10^5 ha) over long time periods, but empirical studies on how microclimate temperature affects forest processes are often restricted to local scales of observation (i.e., typically 10^{-4} to 10^0 ha) and short-term effects. Consequently, there is an inherent scale mismatch of five to six orders of magnitude between the scale of observation and that of ecological interest. Inferring landscape-scale changes from static, plot-scale measurements is challenging, because nonlinear scaling relationships and cross-scale interactions can amplify or dampen effects (Wiens 1989; Peters et al. 2007). Furthermore, forest canopies can be highly diverse across landscapes, resulting in substantial heterogeneity in forest microclimate (Vanwalleghem and Meentemeyer 2009; Vandewiele et al. 2023). Some processes, such as disturbance and recovery, require explicit consideration of spatial patterns (Turner 2010), and disturbances in turn can alter microclimate temperature buffering (Thom et al. 2020; Wolf et al. 2021). Management decisions must also consider landscape scales to explore trade-offs among ecosystem services (e.g., Díaz-Yáñez et al. 2021), account for spatial context when altering species composition and structure (e.g., Mina et al. 2022), and mitigate climate or disturbance impacts on local communities (e.g., Jenerette et al. 2022). Understanding whether and how microclimate buffering at local scales contributes to long-term, broad-scale forest landscape change is therefore critically important for anticipating and managing future forests.

Forest landscape models are ideally suited for addressing this knowledge gap because they simulate landscape patterns as emergent outcomes of ecological processes and interactions occurring at finer spatial grains (DeAngelis and Yurek 2017). Process-based models enable projections of future forest change under no-analog conditions (Gustafson 2013), and improving climate driver representation will make projections more robust. Explicitly accounting for fine-scale microclimate temperature buffering effects could alter landscape scale outcomes, for example by modifying tree regeneration (Dobrowski et al. 2015), leading to longer term shifts in species dominance. Yet, to date microclimate temperature has not been explicitly considered in forest landscape models.

Here we developed a dynamic and computationally efficient microclimate module that incorporates microclimate temperature buffering in the individual-based forest landscape and disturbance model iLand (Seidl et al. 2012a; Rammer et al. 2024). We included microclimate temperature effects on three key forest processes that occur in the understory or near the forest floor, are dependent on temperature, and are simulated explicitly in the current version of iLand. These processes included decomposition of deadwood, litter, and soil organic matter pools; bark beetle development; and tree seedling establishment (i.e., successful first-year germination and survival).

We then used this novel microclimate module to ask, *How does accounting for microclimate temperature buffering affect forest processes from local to landscape scales?* We investigated this question in an illustrative temperate mountain forest landscape covering a broad elevational gradient (Berchtesgaden National Park, Germany). Specifically, we simulated forest and disturbance dynamics under historical climate for 1,000 years, using either daily macroclimate or microclimate temperature as the driver of the three focal subcanopy processes. We then analyzed hypothesized effects on indicators of forest dynamics at three spatial scales (local, meso, and landscape; Table 1). At the local scale (1 ha), we expected cooler microclimate temperatures under dense forest canopies to decrease decomposition (H1a) and bark beetle development rates (H1b) but maintain similar tree regeneration densities (H1c) because increases in cold-preferring species can offset decreases in warm-preferring species. At mesoscales (1-100s of ha), we expected microclimate simulations to enhance effects of disturbance mortality and associated reductions in canopy density on forest processes (H2a-c). Disturbances increase light availability in both microclimate and macroclimate simulations but additionally reduce temperature buffering in microclimate simulations only. We further expected microclimate effects to vary across the elevation ranges of tree species, with the greatest differences at lower or upper range edges relative to median elevations (H3). At the landscape scale (8,645 ha), we expected increased net ecosystem productivity (NEP; H4a) and total carbon (C) storage (H4b) in microclimate versus macroclimate simulations due to decreased decomposition and reduced bark beetle outbreaks (H4c) resulting from slowed beetle development. However, we expected similar forest composition (H4d) because temperature filters are likely less important for determining species occurrence compared to light and seed availability (Table 1).

Materials and methods

Study area

Berchtesgaden National Park is a 20,808 ha topographically complex, temperate landscape (44% of which is forested) ranging from 603-2,713 m in elevation in the northern front range of the European Alps (Figure 1). The climate is cool and wet, mean annual temperature decreases (from 7 to -2 °C) and annual precipitation increases (from 1500 to 2800 mm) with elevation, and precipitation is highest during summer. Lower elevation, submontane to montane forests are dominated by European beech (*Fagus sylvatica* L.); mixed stands of Norway spruce (*Picea abies* (L.) Karst.), silver fir (*Abies alba* Mill.), and beech; or relatively homogeneous and widespread stands of Norway spruce due to historical legacies of timber harvest and replanting. Higher elevation, subalpine forests transition from spruce-dominated to European larch (*Larix decidua* L.), Swiss stone pine (*Pinus cembra* L.), and shrubby patches of dwarf mountain pine (*Pinus mugo* Turra) near the upper treeline (~1,750 m). Dominant forest disturbance agents include European spruce bark beetles (*Ips typographus* L.) and wind, although patch sizes and annual area disturbed tend to be small relative to

Table 1 Spatial and temporal scales used to analyze effects of microclimate temperature buffering, analysis description, forest process and associated indicator, and hypotheses for whether microclimate simulations ("Micro") would have lower (<), higher (>), or similar (~) values compared to macroclimate ("Macro") simulations

Spatial scale	Temporal scale (yrs)	Description	Process	Indicator	Expected effect on process
Local (1 ha)	30	Annual average within dense forested stands (overstory LAI > 4)	Decomposition	Heterotrophic respiration	Micro < Macro (H1a)
			Bark beetle development	Completed beetle generations	Micro < Macro (H1b)
			Tree establishment	Tree regeneration density (stems < 4m height)	Micro ~ Macro (H1c)
Meso (1-10s of ha)	15	Average post- minus pre-disturbance indicator values in disturbance patches (5-15 years since disturbance). Patches represent 10 years of cumulative wind and bark beetle disturbances.	Decomposition	Heterotrophic respiration	Micro > Macro (H2a)
			Bark beetle development	Completed beetle generations	Micro > Macro (H2b)
			Tree establishment	Tree regeneration density	Micro > Macro (H2c)
Meso (100s of ha)	30	Relative difference in regeneration along species-specific elevation ranges [100 m bands centered on the lower bound, median, and upper bound of its elevational regeneration distribution]	Tree establishment	Tree regeneration density for six species	|Difference| at lower or upper bound > |Difference| at median of elevational regeneration distribution (H3)
Landscape (8645 ha)	1000	Average across entire forested landscape (cumulative or averaged over last 30 years)	Decomposition	Net Ecosystem Productivity	Micro > Macro (H4a)
			Decomposition	Total carbon	Micro > Macro (H4b)
			Bark beetle development	Bark beetle disturbance mortality	Micro < Macro (H4c)
			Tree establishment	Tree species composition (basal area share for trees > 4m height)	Micro ~ Macro (H4d)

total forested area (< 1 ha median patch size and < 0.3% annual area disturbed between 1986 and 2020; Senf et al. 2017; Maroschek et al. 2023). Following its establishment in 1978, management ceased in a core zone covering 75% of the park. In the remainder, management activities are restricted to ungulate management, bark beetle mitigation, forest restoration, and cattle grazing in non-forested areas.

Simulation model

The process-based model iLand simulates forest development and landscape change as an emergent outcome of species-specific, individual tree responses to abiotic drivers, disturbances, management, and competition for light (Seidl et al. 2012a; Seidl and Rammer 2024; Rammer et al. 2024). Forest processes such as productivity and biomass allocation, intrinsic and disturbance-related mortality, seed production and dispersal, and tree establishment are modeled from basic ecological principles (*sensu* Gustafson 2013). Seedlings and saplings are simulated as regeneration cohorts until reaching 4 m in height, when they are recruited as individual trees. Tree crowns shade their neighbors and the subcanopy environment, modifying microclimate light availability (2 m horizontal resolution), but until this study microclimate temperature buffering effects had not yet

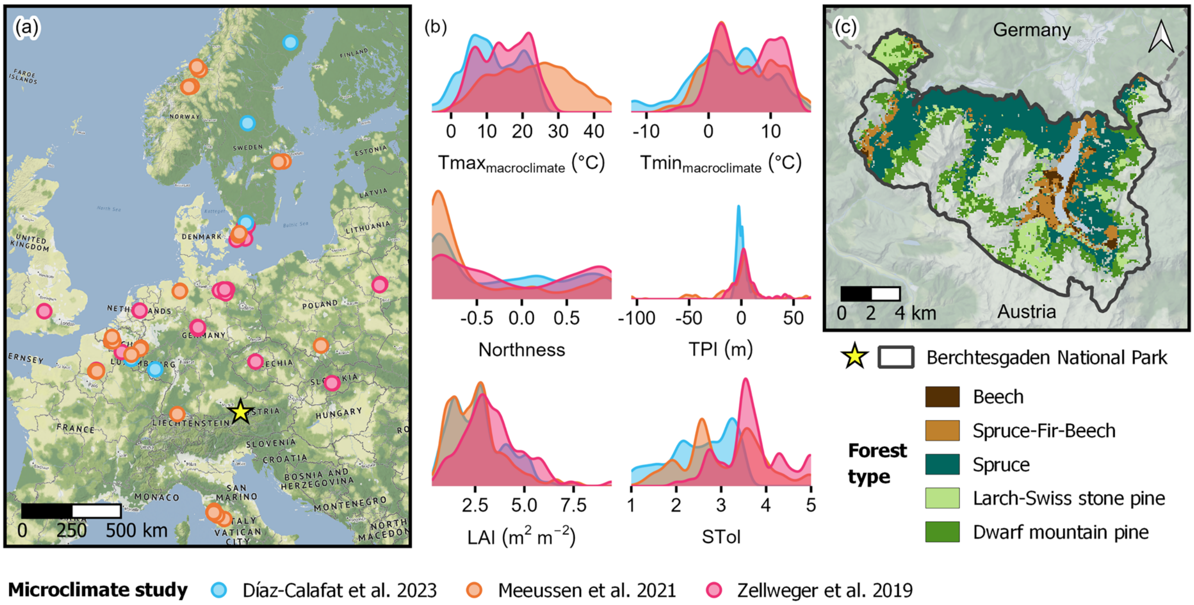

Fig. 1 (a) Location of plots (n = 497, circles) across Europe from three studies where *in situ* microclimate data were collected in coniferous and broadleaved forests. Data were used here to fit empirical temperature offset models. The location of Berchtesgaden National Park is indicated by a star. (b) Density plots showing the distribution of predictor variables (see Table 2 for descriptions) across the three studies. (c) Forest simulation landscape, which includes all forested areas in Berchtesgaden National Park in Germany, and contemporary forest types. Map credits © Natural Earth, OpenMapTiles, OpenStreetMap, QGIS, Stadia Maps, Stamen Design. Beech: *Fagus sylvatica*, Spruce: *Picea abies*, Fir: *Abies alba*, Larch: *Larix decidua*, Swiss stone pine: *Pinus cembra*, Dwarf mountain pine: *Pinus mugo*

been incorporated. Carbon is tracked in live, dead, and soil pools, with photosynthesis, respiration, disturbance, management, and decomposition affecting fluxes among pools and to the atmosphere. Spatially explicit disturbance modules include abiotic disturbances such as wind (Seidl et al. 2014) and biotic disturbances such as bark beetles (Seidl and Rammer 2017). Bark beetle disturbances consider the life cycle of the beetle, climate-driven outbreak initiation and interactions with windthrow, spatially explicit spread, species identity and size of potential host trees, and stress-related susceptibility to colonization. Detailed model documentation is available at https://iland-model.org (Seidl and Rammer 2024).

Empirical temperature offset models

We fit linear mixed effects models (LMMs) predicting microclimate temperature offset (°C) using data from 497 widely distributed field plots in European coniferous and broadleaved forests from three studies (Zellweger et al. 2019; Meeussen et al. 2021; Díaz-Calafat et al. 2023; Figure 1; Table S1). In each field plot, daily minimum and maximum microclimate temperature were measured at ~1m height for one to two years between 2017 and 2021, and macroclimate temperature was either acquired from a nearby weather station or measured in nearby open areas with no canopy cover (generally a nearby grassland site). Microclimate temperature offsets were calculated as microclimate minus macroclimate temperature (Equations S1-S2), meaning negative values represent cooler forest understory temperatures. Temperature data were previously reviewed and cleaned in each study, and we performed additional quality checks to identify snow days (i.e., when the microclimate sensor was covered in snow), erroneous time periods, and extreme outliers. To further reduce outlier effects and improve data normality while maintaining seasonal variation, we calculated the monthly average of daily minimum and maximum temperature offsets (hereafter, "average daily"). Separate LMMs were then fit to predict average daily minimum and maximum temperature offsets (n = 7,755 observations). Predictors included macroclimate temperature, topography [northness, topographic position index (TPI)], and forest structure and composition [overstory leaf area index (LAI), overstory shade tolerance as a proxy for species composition and differences in canopy architecture] as fixed effects and study ($n = 3$) as a random intercept effect to account for methodological or other differences among studies not captured by the fixed effects (Figure 1b, Table 2, Table S1). Predictors, including study, were not highly correlated (all squared scaled generalized variance inflation factors < 1.6; Fox 2016; see Supporting Information for additional detail).

Microclimate module and effects on forest processes

We predicted average daily minimum and maximum microclimate temperature offset in iLand at 10m spatial resolution using the empirically derived temperature offset models and dynamically derived predictor variables from iLand (Table 2). Predictors were truncated to the maximum and minimum values used in model fitting to avoid extrapolating beyond the range of values used to train the models. We averaged minimum and maximum offset to derive average daily mean microclimate temperature offset. Temperature offsets were updated monthly for each 10m cell but were added to daily macroclimate temperature to match the time step of iLand, meaning microclimate temperature varied daily in the simulation model.

To evaluate simulated microclimate buffering in iLand, we compared seasonal variability, differences among forest types, and spatial patterns of temperature offsets with ecological expectations and with an independent, wall-to-wall microclimate dataset. This dataset consisted of Berchtesgaden summer temperature offset maps derived by combining *in situ* microclimate and macroclimate observations from 2021 with LiDAR-derived metrics of forest structure and topography (Vandewiele et al. 2023). Because daily downscaled (100 m) historical macroclimate data used in iLand were only available for 1980–2009 (Thom et al. 2022), evaluation simulations used contemporary forest and topographic conditions with macroclimate from a year representing average historical mean annual temperature for the landscape (5.7 °C, in 1988).

We simulated effects of microclimate temperature buffering on three temperature-dependent processes that occur in the forest understory: decomposition, bark beetle development, and tree establishment. These processes were already implemented and tested

Table 2 Variables used in average daily microclimate temperature offset models

Variable	Short name	Units	Description
Fixed effects			
Average daily minimum macroclimate temperature	$Tmin_{macroclimate}$	°C	Monthly average of daily minimum free-air temperature; only used in predicting minimum offset
Average daily maximum macroclimate temperature	$Tmax_{macroclimate}$	°C	Monthly average of daily maximum free-air temperature; only used in predicting maximum offset
Northness	Northness	dim[-1,1]	Cosine of topographic aspect
Topographic position index	TPI	m	Relative topographic position calculated as plot elevation minus mean elevation within a 500m radius
Leaf area index	LAI	$m^2\ m^{-2}$	Projected leaf area per unit area (one-sided), calculated as the sum of foliage biomass times specific leaf area across all individual trees. Updated annually in iLand.
Shade tolerance	STol	dim[1,5]	Weighted mean shade tolerance across tree species, weighted by relative basal area. 1=very light-demanding, 5=very shade tolerant. Updated annually in iLand.
Random intercept effect			
Study	Study	3 levels	Categorical variable, name of the study associated with each microclimate dataset (see Figure 1)

in previous versions of iLand; in the new microclimate version of the model, affected processes use daily microclimate rather than macroclimate temperature as inputs. Forest processes occurring within or near the top of the canopy, such as tree primary production, were driven by macroclimate temperature in all simulations. Macroclimate temperatures in iLand refer to free-air temperature at 2 m height and 100 m horizontal resolution, derived from interpolated historical weather station data (Thom et al. 2022). To calculate microclimate temperature in iLand, offsets were averaged at 100 m spatial resolution across stockable 10m cells (i.e., excluding areas such as rocks or water bodies that are unable to become forested), and then added to macroclimate temperature (Equations S1-S2).

Decomposition rates of snags, downed wood, litter, and soil organic matter are simulated based on first order decay kinetics in iLand. The reference decay rate is sensitive to a climate modifier that accounts for temperature and moisture (Adair et al. 2008; Seidl et al. 2012b). This modifier affects both the transition rate between carbon pools (e.g., downed wood to soil) and the rate of heterotrophic respiration to the atmosphere (Kätterer and Andrén 2001). To account for temperature buffering effects, the microclimate module calculates this modifier from mean microclimate instead of macroclimate temperature.

In Central European forests, iLand simulates the dynamics of the European spruce bark beetle *Ips typographus* (henceforth "bark beetle" for brevity). Bark beetles can produce multiple generations per year, with bark temperature influencing development rates and sister brood initiation (Baier et al. 2007). In the newly developed microclimate module, bark temperature is calculated from maximum microclimate instead of maximum macroclimate air temperature, and overwintering success is based on minimum microclimate rather than minimum macroclimate temperature (see Seidl and Rammer 2017 for the equations representing the respective processes). Other climate-sensitive aspects of bark beetle spread and outbreak intensity, such as outbreak initiation and host tree susceptibility, are driven by macroclimate temperature, summer precipitation, and drought stress.

Successful tree establishment in iLand relies on passing multiple, species-specific abiotic filters. These filters include minimum winter temperature, winter chilling requirements, and growing degree days, which act as thresholds either allowing or preventing establishment (Nitschke and Innes 2008). Other abiotic conditions, including soil water availability and growing season frost events, also modify establishment probabilities if thresholds are met (see Seidl et al. 2012b and Hansen et al. 2018 for a detailed description). In the newly developed microclimate module, abiotic filters are calculated from daily minimum (minimum winter temperature, growing season frost) or mean (winter chilling requirements, growing degree days) microclimate rather than macroclimate temperature.

Initial conditions and simulation experiment

Contemporary forest conditions (year 2020); historical climate, soils, and topography; wind and bark beetle disturbance regimes; and tree species parameters for Berchtesgaden National Park were derived and rigorously evaluated by Thom et al. (2022) and have been used in multiple studies (Albrich et al. 2022; Dollinger et al. 2023; Braziunas et al. 2024). To assess effects of microclimate temperature buffering from local to landscape scales, we simulated 1,000 years of forest development under historical climate and disturbances, with no forest management, and starting from contemporary forest conditions including all major and most minor tree species in Berchtesgaden National Park. Simulations either used macroclimate or microclimate temperature as drivers of decomposition, bark beetle development, and tree establishment processes. We simulated 10 replicates of each condition (macroclimate or microclimate) to account for variation due to probabilistic processes in iLand (Rammer et al. 2024). To further isolate the importance of macroclimate versus microclimate temperature as the driver of forest dynamics, each replicate followed a randomly selected sequence of climate years and wind events drawn from the previously compiled historical data representing the period 1980 to 2009 (Thom et al. 2022).

Analyses across scales

We analyzed the effect of microclimate temperature buffering on indicators of the three focal forest processes by comparing simulations driven with macroclimate or microclimate at three spatial scales and variable temporal scales (Table 1; see Supporting Information for additional detail). At local scales, we compared forest process indicators in dense forested stands. At mesoscales, we quantified disturbance effects as the post- minus pre-disturbance indicator value within disturbance patches. Also at mesoscales, differences in tree establishment along species-specific elevation ranges were assessed for a subset of representative species varying in elevational range and temperature sensitivity: beech and silver fir (submontane-montane zone, warm preferring), spruce and Swiss stone pine (subalpine, cold preferring), and sycamore maple (*Acer pseudoplatanus* L.) and larch (montane and subalpine, respectively, temperature indifferent; Ellenberg and Leuschner 2010). At the landscape scale, we compared NEP, carbon storage, disturbance mortality, and tree species composition after 1000 years of forest development (Table 1). We then compared relative differences in landscape-scale indicators between the first and last 30 simulation years and with local-scale indicators to consider how microclimate effects changed over time and across scales. Because data were generated via a simulation experiment, comparisons prioritized ecologically meaningful interpretations such as relative differences between mean indicator values and variability based on standard errors, rather than tests of statistical significance (White et al. 2014).

Results

Empirical temperature offset models

In order of predictor importance, buffered (i.e., warmer) minimum microclimate temperatures were associated with higher TPI, more northerly aspects, lower shade tolerance, cooler minimum macroclimate temperatures, and higher LAI (Equation S3, Table 3). Model fit for average daily minimum temperature offset was conditional $R^2_c = 0.24$ (full model), marginal $R^2_m = 0.07$ (fixed effects only), and root-mean-squared-error (RMSE) = 1.4 °C (Figure S6a). In order of predictor importance, buffered (i.e., cooler) maximum microclimate temperatures were associated with warmer maximum macroclimate temperatures, higher LAI, more northerly aspects, lower shade tolerance, and lower TPI (Equation S4, Table 4). Model fit for average daily maximum temperature offset was conditional $R^2_c = 0.47$, marginal $R^2_m = 0.29$, and RMSE = 2.7 °C (Figure S6b). Models represented seasonal variability in microclimate temperature buffering well (Figure S6c-d).

Dynamically simulated temperature offsets in iLand

Daily temperature offsets averaged -0.7 °C for maximum, 0.1 °C for mean, and 0.8 °C for minimum temperatures across the entire forested landscape during a year with average historical climate conditions (mean of 864,466 observations at 10 m spatial resolution; Figure 2a-c; Table S2). Relative to maximum and

Table 3 Linear mixed effects model coefficients and random intercept effect standard deviation for average daily minimum temperature offset models, fit to $n = 7{,}755$ observations

Variable	Estimate	Standard error (fixed effects) or standard deviation (random intercept effect)	t	p
Fixed effects				
(Intercept)	1.4570	0.3877	3.7590	0.03
TPI	0.0158	0.0009	18.1540	$< 2.00 \times 10^{-16}$
Northness	0.2627	0.0237	11.0990	$< 2.00 \times 10^{-16}$
STol	-0.2031	0.0224	-9.0560	$< 2.00 \times 10^{-16}$
$Tmin_{macroclimate}$	-0.0248	0.0029	-8.6360	$< 2.00 \times 10^{-16}$
LAI	0.0227	0.0127	1.7960	0.07
Random intercept effect				
Study	–	0.6614	–	–

$Tmin_{macroclimate}$ Average daily minimum macroclimate temperature: *LAI* Leaf area index; *STol* Shade tolerance; *TPI* Topographic position index

Table 4 Linear mixed effects model coefficients and random intercept effect standard deviation for average daily maximum temperature offset models, fit to $n = 7{,}755$ observations

Variable	Estimate	Standard error (fixed effects) or standard deviation (random intercept effect)	t	p
Fixed effects				
(Intercept)	0.9767	0.9428	1.0360	0.37
$Tmax_{macroclimate}$	-0.1932	0.0034	-57.3680	$< 2.00 \times 10^{-16}$
LAI	-0.3948	0.0250	-15.7920	$< 2.00 \times 10^{-16}$
Northness	-0.5729	0.0466	-12.2910	$< 2.00 \times 10^{-16}$
STol	0.4419	0.0442	9.9900	$< 2.00 \times 10^{-16}$
TPI	0.0140	0.0017	8.0790	7.51×10^{-16}
Random intercept effect				
Study	–	1.6145	–	–

$Tmax_{macroclimate}$ Average daily maximum macroclimate temperature, *LAI* Leaf area index, *STol* Shade tolerance, *TPI* Topographic position index

mean macroclimate temperatures, forests tended to warm microclimate temperatures in the winter (average offset = 0.8 and 0.9 °C for maximum and mean, respectively) and cool microclimate temperatures in the summer (-2.2 and -0.8 °C), with spring and autumn temperature offsets falling in between these extremes. Forests consistently tended to warm minimum microclimate relative to macroclimate temperatures across the full year.

Microclimate temperature buffering differed among forest types and across the landscape, and simulated mean summer offsets during an average historical climate year (1988) aligned with independent offset maps derived from field data and LiDAR collected in 2021 (Spearman's ρ = 0.47; Figure S8). Mean summer microclimate temperatures were cooled the most in beech-dominated forests (average offset = -1.3 °C), followed by spruce-fir-beech and spruce (both -1.0 °C), dwarf mountain pine (-0.4 °C), and larch-Swiss stone pine forest types (-0.3 °C; Figure 2e). Trends were similar for maximum and minimum temperature offsets, except that spruce forests cooled maximum temperatures slightly more than beech forests (-2.6 versus -2.5 °C for spruce and beech, respectively; Figure 2d) and warmed minimum temperatures more than spruce-fir-beech forests (0.6 versus 0.2 °C for spruce and spruce-fir-beech, respectively; Figure 2f). Lower (i.e., more negative, cooler) temperature offsets occurred at lower elevations and valley bottoms whereas higher (i.e., more positive, warmer) offsets occurred at higher elevations and exposed ridges (Figure 2g–i).

Local-scale effects

In dense forested stands, annual heterotrophic respiration was 2% lower (9.25 vs. 9.48 Mg C ha^{-1}), the number of completed bark beetle generations 20% lower (1.37 vs. 1.72 generations), and tree regeneration density 3% lower (10,463 vs. 10,820 stems ha^{-1}) in microclimate compared to macroclimate simulations (Figure 3). Regeneration composition shifted in dense forested stands, with slightly higher proportions of some subalpine species and slightly lower proportions of some submontane to montane species in microclimate versus macroclimate simulations (Figure S9).

Mesoscale effects

Variability among patches exceeded variability between macroclimate and microclimate simulations for post- minus pre-disturbance changes in heterotrophic respiration rates and tree regeneration densities (Figure S10). However, including microclimate temperature buffering more consistently enhanced post-disturbance bark beetle development (mean change 0.17 versus 0.09 generations ha^{-1} and increases in 46% versus 32% of patches in microclimate versus macroclimate simulations, respectively). Disturbance patch numbers and sizes differed between macroclimate (283 patches, 1-59 ha in size) and microclimate simulations (165 patches, 1-49 ha).

Microclimate temperature-driven differences in tree regeneration varied among representative

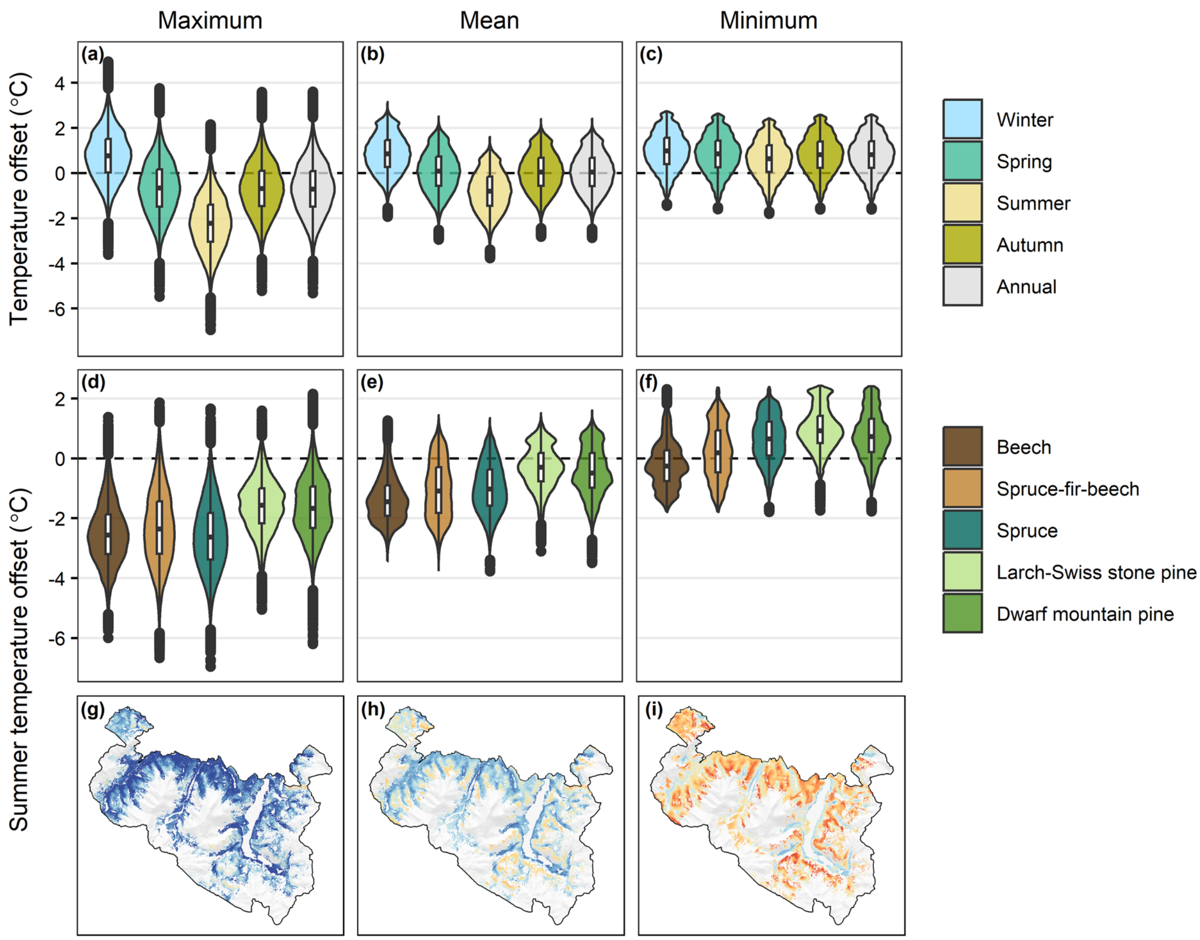

Fig. 2 Simulated maximum, mean, and minimum temperature offsets in Berchtesgaden National Park using the newly developed microclimate module in iLand, based on contemporary forest conditions and a year with average historical climate conditions. (a-c) Seasonal and annual temperature offsets across all forested cells (864,466 observations per season at 10 m spatial resolution). (d-f) Summer (June-August) temperature offsets by forest type. (g-i) Maps of summer temperature offsets (values truncated to -3 and 3). Temperature offsets are microclimate minus macroclimate temperature. Beech: *Fagus sylvatica*, Spruce: *Picea abies*, Fir: *Abies alba*, Larch: *Larix decidua*, Swiss stone pine: *Pinus cembra*, Dwarf mountain pine: *Pinus mugo*

species and along their elevational ranges (Figure 4). Four of the six species (Swiss stone pine, larch, spruce, beech) responded more to microclimate effects at the lower or upper bounds relative to median values within their elevation range, and most species tended to increase in density at higher elevations. Subalpine species usually increased in regeneration density (Figure 4a–c), whereas submontane and montane species decreased at lower and median elevations (Figure 4d–f). Within these elevation zones, temperature-indifferent species (larch, sycamore maple) tended to be less sensitive than other species to microclimate effects on regeneration density.

Landscape-scale effects

After 1,000 years, total carbon and cumulative NEP were higher (by 2 and 21%, respectively) and forest species composition differed in microclimate versus macroclimate simulations (Figures 5, S11-S12). Increases in total carbon were primarily driven by increased soil carbon (7.10 Mg C ha^{-1}) and partially offset by decreased live carbon (-1.64 Mg C ha^{-1}). When

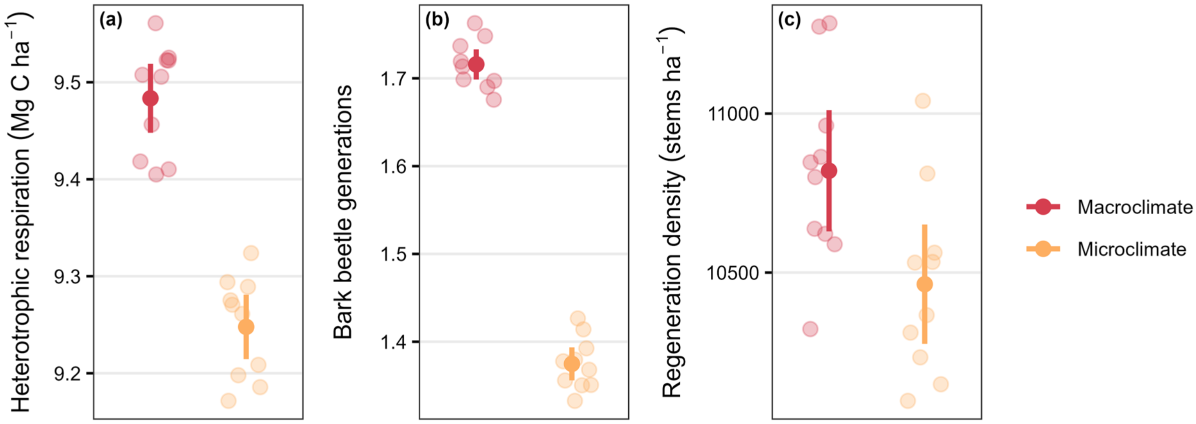

Fig. 3 Local scale indicators of forest processes for simulations without (macroclimate, red) versus with (microclimate, yellow) temperature buffering included in the model. (a) Heterotrophic respiration as an indicator of decomposition, (b) completed bark beetle generations as an indicator of bark beetle development, and (c) regeneration density for stems < 4 m height as an indicator of tree establishment. Values are the annual average for dense forested stands (LAI > 4) over the first 30 simulation years. Solid points: mean across all replicates, error bars: two standard errors, jittered shaded points: mean value for each simulated replicate (n = 10 replicates)

microclimate temperature buffering was included, basal area share increased for dominant subalpine species (from 7 to 12% for larch and 46 to 55% for spruce) and decreased for dominant submontane-montane species (from 12 to 9% for silver fir and 34 to 22% for beech). Cumulative bark beetle-caused tree mortality was 21% lower in microclimate versus macroclimate simulations but windthrows more than compensated for this decline, resulting in a 3% increase in total disturbance mortality (Figure 5, S11-S12).

Relative differences between microclimate and macroclimate simulations tended to be lower in magnitude for landscape versus local-scale indicators of decomposition and tree establishment (Figure S13). However, relative decreases in bark beetle-caused mortality at the landscape scale were of greater magnitude (-45%) than decreases in bark beetle development rates at the local scale (-16%). Landscape scale differences between microclimate and macroclimate simulations increased over time for total carbon and species basal area, but not for annual NEP or disturbance mortality (Figure S12).

Discussion

We developed the first explicit and dynamic implementation of microclimate temperature buffering in a forest landscape simulation model and found that microclimate effects cannot be neglected for simulated forest dynamics. Local effects of buffered subcanopy temperatures scaled up nonlinearly, underlining the utility of using complex simulation models for dynamic upscaling in space and time. Spatially, microclimate effects at local scales could not simply be added up to estimate landscape scale outcomes. Temporally, microclimate effects were not static, as interacting drivers (e.g., disturbances) and cross-scale feedbacks were either amplifying or dampening. By explicitly modeling microclimate temperature buffering in a process-based forest landscape model, we provide a tool that is well suited for investigating critical ecological challenges in the 21st century.

Simulated microclimate temperature offsets aligned with expectations

Microclimate temperature offset predictions echoed ecological expectations, and offset magnitudes were within the range of empirical observations in temperate forests (De Frenne et al. 2019). Responses to predictors were consistent with previous studies that found higher buffering with increasing canopy density (von Arx et al. 2013; Zellweger et al. 2019) and under more extreme macroclimate temperatures (De Frenne et al. 2019; Thom et al. 2020). Cooler microclimates

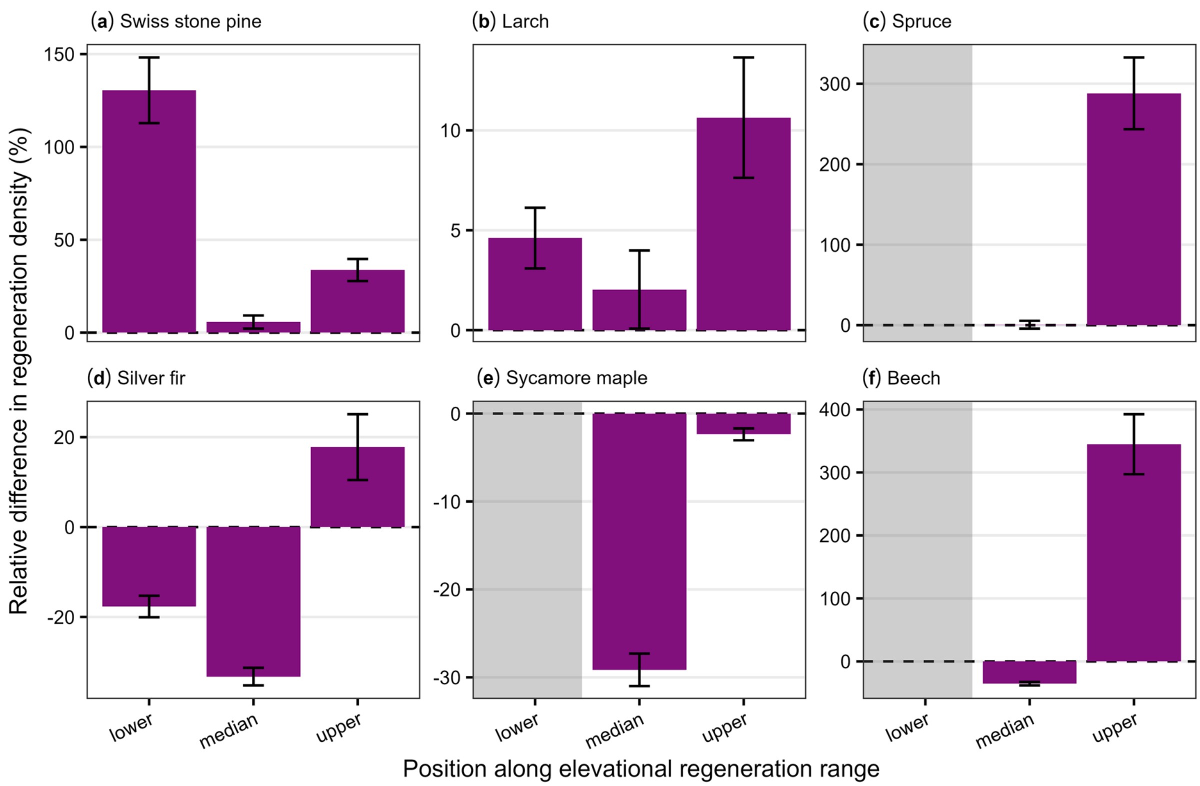

Fig. 4 Relative difference in regeneration density for six representative tree species along their elevation ranges (100 m bands centered on the lower bound, median, and upper bound of their elevational distribution). Positive values indicate increased regeneration when microclimate temperature buffering is included in the model. Bar height: mean, error bars: two standard errors ($n = 10$ replicates), gray boxes: excluded from analysis because they fell below the minimum landscape elevation. Swiss stone pine: *Pinus cembra*, Larch: *Larix decidua*, Spruce: *Picea abies*, Silver fir: *Abies alba*, Sycamore maple: *Acer pseudoplatanus*, Beech: *Fagus sylvatica*.

at lower topographic positions reflected cold air pooling dynamics (Pastore et al. 2022). Seasonal trends aligned with empirical studies, finding enhanced cooling of maximum temperatures during summer and lower seasonal variability for minimum temperature buffering (Zellweger et al. 2019; Meeussen et al. 2021). However, variance explained by fixed effects was low, especially for minimum temperature offsets. Differences among the three study datasets (e.g., in instrumentation, macroclimate data source, and range of predictor values) likely contributed to poor model performance.

Simulated summer microclimate temperature offsets aligned well with independent offset maps derived from field data and LiDAR (Vandewiele et al. 2023). This independent dataset was not used to train the model, yet the relative ranking of forest types and hotspots of highest and lowest buffering capacity were similar for maximum and mean offsets. Differences between datasets were likely primarily due to different microclimate measurement height. Temperatures close to the ground (15 cm for independent data) may diverge from 1 m height measurements (as simulated in iLand) due to dense understory vegetation, differential air mixing, and closer proximity to the soil surface where radiant heat transfer occurs (Geiger 1950; Campbell and Norman 1998). Overall based on this independent data comparison, we conclude that the temperature offsets simulated in this study are robust and consistent with empirically derived expectations for microclimate temperature buffering.

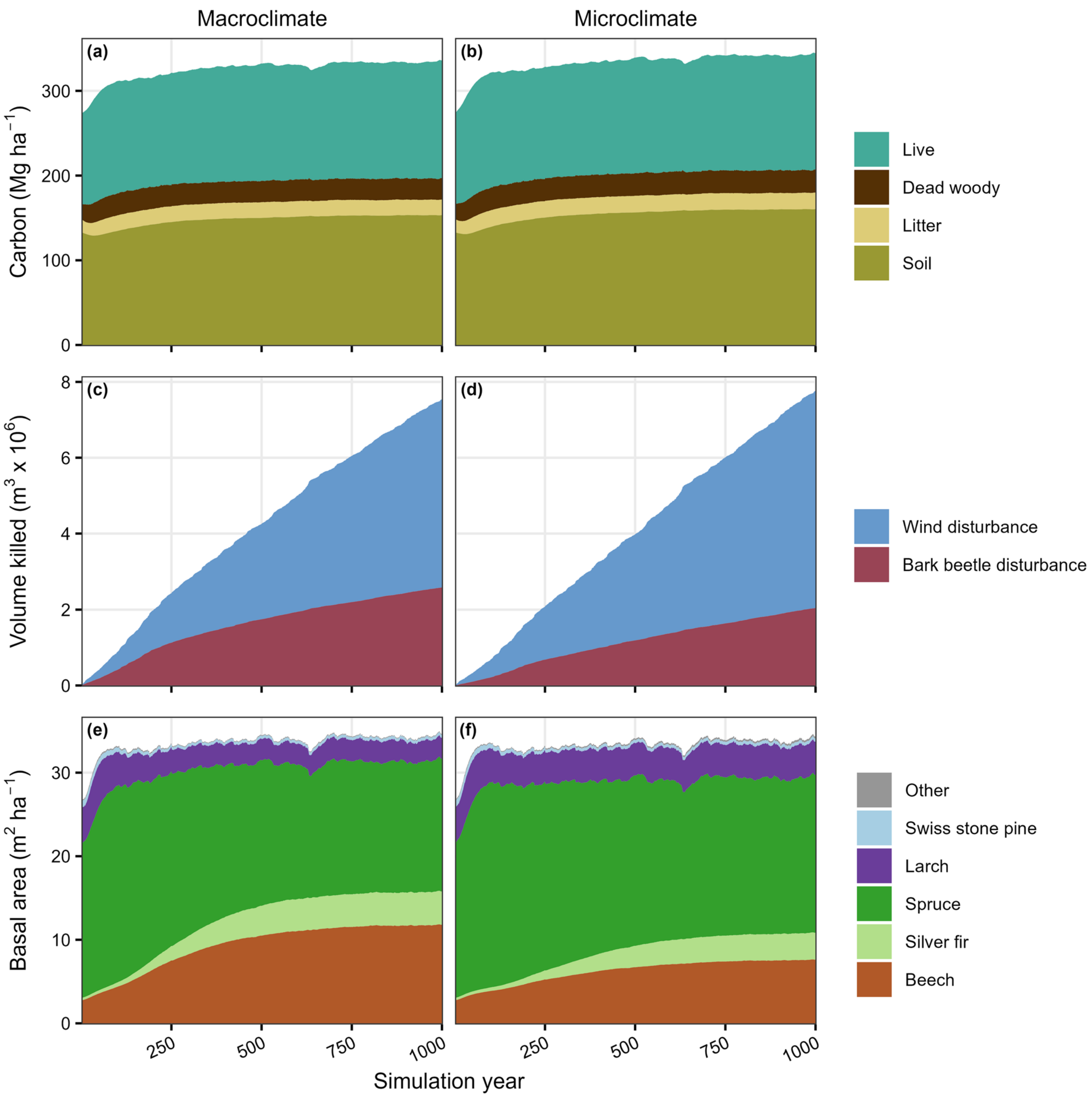

Fig. 5 Landscape scale trajectories for (a-b) total carbon and carbon pools, (c-d) cumulative disturbance mortality due to wind and bark beetles, and (e-f) tree species basal area, without (left) or with (right) microclimate temperature buffering effects included in the model. Plots show the mean value from 10 simulated replicates. Beech: *Fagus sylvatica*, Spruce: *Picea abies*, Fir: *Abies alba*, Larch: *Larix decidua*, Swiss stone pine: *Pinus cembra*, Dwarf mountain pine: *Pinus mugo*

Microclimate temperature buffering mattered across scales

At local scales, decomposition and bark beetle development decreased as expected (H1a-H1b; see Table 1 for hypotheses) in dense forested stands when driven by microclimate rather than macroclimate temperature. Counter to our expectations (H1c), tree regeneration densities also tended to decrease, suggesting that cooler maximum and mean temperatures drove overall responses (e.g., by reducing the likelihood of meeting growing degree day thresholds) more than warmer minimum temperatures (e.g., by reducing growing season frost events). Shifts in tree regeneration composition imply that some species benefit more from microclimate temperature buffering than others due to species-specific traits (Dobrowski et al. 2015).

At mesoscales, high variability among disturbance patches overwhelmed differences between microclimate and macroclimate simulations for all processes except bark beetle development (H2a-c). Temperature is only one factor influencing post-disturbance dynamics, and processes may be more sensitive to other disturbance-mediated factors such as amount and arrangement of dead woody biomass (e.g., heterotrophic respiration; Harmon et al. 2011), light availability (e.g., tree seedling survival and growth; Xu et al. 2023), and biotic legacies (e.g., seed supply; Gill et al. 2022). Furthermore, if disturbance severity is low, canopy gaps are small, or residual structures remain – as is frequently the case in our study landscape – disturbance effects on temperature buffering may be less pronounced (Abd Latif and Blackburn 2010; Carlson et al. 2021). Microclimate effects on tree establishment along elevational ranges generally aligned with expectations (H3). Positive effects at higher elevations suggest most species benefited from being released from minimum temperature and frost limitations.

At the landscape scale, total carbon and cumulative NEP increased as expected (H4a-b), but forest composition shifted more substantially than expected (H4d) when driven by microclimate rather than macroclimate temperature. Compositional changes highlight the role of intact forest canopies and variable topography in creating climatic conditions that favor certain species (Dobrowski et al. 2015). Shifts in landscape scale carbon storage and cycling suggest cascading effects of microclimate-driven processes on the climate regulating function of forests (De Frenne et al. 2021; Pastore et al. 2022). In addition to removing live woody carbon, forest loss could accelerate carbon losses from soil and dead pools if decomposition rates increase with warmer free-air temperatures. Bark beetle development rates were dampened as expected (H4c) but, perhaps surprisingly, did not translate into overall reductions in disturbance mortality because increasing wind disturbances more than compensated for declining bark beetle disturbances. However, this trade-off is ecologically reasonable; the dense, homogeneous stands of large Norway spruce that dominate this landscape are susceptible to both bark beetle and wind disturbances (Stritih et al. 2021). Previous studies have found similar compensatory disturbance dynamics in forests of Central Europe (Dobor et al. 2020).

Limitations and future directions

We only considered microclimate buffering effects on temperature in this study. However, forest canopies already influence light availability and water cycling in iLand simulations (Seidl et al. 2012a). Some processes, such as decomposition, are therefore already influenced by canopy-mediated effects on precipitation and potential evapotranspiration (Adair et al. 2008). Additionally, other climate-sensitive processes occur underneath forest canopies. For example, future model development could explore microclimate effects on surface fuel moisture and associated dynamics of fire ignition, spread, and severity (Rothermel 1983).

Our aim was to identify a generalizable, robust, dynamic, and computationally efficient approach for representing microclimate temperature effects on forest processes and landscape outcomes (i.e., to find the Medawar zone of optimal model complexity; Grimm et al. 2005). For this reason, we used a simple empirical equation to predict temperature offsets rather than a process-based approach rooted in environmental biophysics (e.g., as in microclimc; Maclean and Klinges 2021). We capitalize on the strengths of a process-based forest model such as iLand by simply substituting microclimate for macroclimate temperature for focal processes, allowing effects to propagate across spatial scales and over time, and annually updating temperature buffering based on dynamic changes in forest structure and composition. This study is meant to contrast outcomes if realistic microclimate temperature offsets are used as the proximal drivers of forest understory processes, not to provide an actual projection of change for this forest landscape. Our empirical model is calibrated for topographically complex, temperate forest landscapes in Europe, and users in other regions should test and refine models as needed and evaluate whether tree species regeneration parameters need to be updated. Some influential drivers (e.g., moderating effects of local water balance on temperature buffering; von Arx et al. 2013; Davis et al. 2019) were less relevant in this landscape but could be considered in future model development.

Simulating future forests

Our findings suggest that forest models should explicitly consider microclimate temperature to improve inferences about the future (De Frenne et al. 2021). Disregarding temperature buffering may lead to overestimation of extinction risks due to climate change (Lenoir et al. 2017) and underprediction of lagged biodiversity change in subcanopy forest communities (Zellweger et al. 2020). Forests may maintain favorable temperature conditions for many forest-dependent species under increasingly extreme climate change, potentially giving species more time to move to new habitats (i.e., as stepping-stones) or sustaining habitats for relatively immobile plant and animal species (i.e., as holdouts or microrefugia; Hannah et al. 2014). Because forest management alters canopy density and structure, accounting for resulting impacts on microclimate temperature can improve our understanding of how management affects forest processes from local to landscape scales (Chen et al. 1999; Menge et al. 2023). Forests cool microclimates more when macroclimate temperatures are hotter, suggesting that microclimate effects will be even more pronounced under future climate change if forest cover is maintained (De Lombaerde et al. 2022). Here, we present a new microclimate module for a freely available, process-based forest landscape model that allows us to explore a wide variety of climate, disturbance, and forest management scenarios and quantify the implications of temperature buffering on future forests and the services they provide.

Acknowledgements We thank four anonymous reviewers for constructive reviews and comments that improved this manuscript.

Author contributions K.H.B.: Conceptualization, Data curation, Formal analysis, Investigation, Methodology, Software, Visualization, Writing – Original Draft Preparation; W.R.: Conceptualization, Data curation, Methodology, Software, Writing – Review & Editing; P.D.F.: Data curation, Writing – Review & Editing; J.D.C.: Data curation, Writing – Review & Editing; P.-O.H.: Data curation, Writing – Review & Editing; C.S.: Conceptualization, Writing – Review & Editing; D.T.: Conceptualization, Software, Writing – Review & Editing; F.Z.: Data curation, Methodology, Writing – Review & Editing; R.S.: Conceptualization, Funding acquisition, Methodology, Project administration, Software, Supervision, Writing – Original Draft Preparation

Funding Open Access funding enabled and organized by Projekt DEAL. Funding support for this project was provided by the European Research Council under the European Union's Horizon 2020 research and innovation program (Grant Agreement 101001905 FORWARD, 757833 FORMICA, and 614839 PASTFORWARD). JDC and POH were supported by the C. F. Lundströms stiftelse (CF2019-0030) from the Royal Swedish Academy of Agriculture and Forestry, as well as Crafoordska stiftelsen 20190675 and 20200544. CS acknowledges support from the German Research Foundation (509915426). FZ was supported by the Swiss National Science Foundation (Grant Number 193645). DT acknowledges support from the "Fachagentur Nachwachsende Rohstoffe" (FNR), under the auspices of the Federal Ministry of Food and Agriculture (BMEL) (Grant Number 2224NR098X).

Data availability Data and code that support the findings of this study, including source code for the iLand version used in this study, are openly available at the Environmental Data Initiative: https://doi.org/10.6073/pasta/06059a68275f7d0c56c9055df3288aac. The individual-based forest landscape and disturbance model iLand is freely available, open source, and fully documented (https://iland-model.org/).

Declarations

Conflict of interests The authors declare no competing interests.

References

Abd Latif Z, Blackburn GA (2010) The effects of gap size on some microclimate variables during late summer and autumn in a temperate broadleaved deciduous forest. Int J Biometeorol 54:119–129.

Adair EC, Parton WJ, Del Grosso SJ et al (2008) Simple three-pool model accurately describes patterns of

long-term litter decomposition in diverse climates. Global Change Biol 14:2636–2660.
Albrich K, Seidl R, Rammer W, Thom D (2022) From sink to source: Changing climate and disturbance regimes could tip the 21st century carbon balance of an unmanaged mountain forest landscape. For Int J for Res 95:742.
Baier P, Pennerstorfer J, Schopf A (2007) PHENIPS—A comprehensive phenology model of Ips typographus (L.) (Col., Scolytinae) as a tool for hazard rating of bark beetle infestation. For Ecol Manag 249:171–186.
Braziunas KH, Geres L, Richter T et al (2024) Projected climate and canopy change lead to thermophilization and homogenization of forest floor vegetation in a hotspot of plant species richness. Global Change Biol 30:e17121.
Campbell GS, Norman JM (1998) An Introduction to Environmental Biophysics. Springer-Verlag, New York, NY
Carlson AR, Sibold JS, Negrón JF (2021) Wildfire and spruce beetle outbreak have mixed effects on below-canopy temperatures in a Rocky Mountain subalpine forest. J Biogeogr 48:216–230.
Chen J, Saunders SC, Crow TR et al (1999) Microclimate in forest ecosystem and landscape ecology: Variations in local climate can be used to monitor and compare the effects of different management regimes. Bioscience 49:288–297.
Davis KT, Dobrowski SZ, Holden ZA et al (2019) Microclimatic buffering in forests of the future: the role of local water balance. Ecography 42:1–11.
De Frenne P, Zellweger F, Rodríguez-Sánchez F et al (2019) Global buffering of temperatures under forest canopies. Nature Ecol Evol 3:744–749.
De Frenne P, Lenoir J, Luoto M et al (2021) Forest microclimates and climate change: Importance, drivers and future research agenda. Global Change Biol 27:2279–2297.
De Lombaerde E, Vangansbeke P, Lenoir J et al (2022) Maintaining forest cover to enhance temperature buffering under future climate change. Sci Total Environ 810:151338.
DeAngelis DL, Yurek S (2017) Spatially explicit modeling in ecology: a review. Ecosystems 20:284–300.
Díaz-Calafat J, Uria-Diez J, Brunet J et al (2023) From broadleaves to conifers: The effect of tree composition and density on understory microclimate across latitudes. Agric for Meteorol 341:109684.
Díaz-Yáñez O, Pukkala T, Packalen P et al (2021) Multi-objective forestry increases the production of ecosystem services. For Int J for Res 94:386–394.
Dobor L, Hlásny T, Rammer W et al (2020) Is salvage logging effectively dampening bark beetle outbreaks and preserving forest carbon stocks? J Appl Ecol 57:67–76.
Dobrowski SZ, Swanson AK, Abatzoglou JT et al (2015) Forest structure and species traits mediate projected recruitment declines in western US tree species. Global Ecol Biogeogr 24:917–927.
Dollinger C, Rammer W, Seidl R (2023) Climate change accelerates ecosystem restoration in the mountain forests of Central Europe. J Appl Ecol 60:2665–2675.
Ellenberg H, Leuschner C (2010) Vegetation Mitteleuropas mit den Alpen. In ökologischer, dynamischer und historischer Sicht, 6th edn. UTB, Stuttgart
Fox J (2016) Applied regression analysis and generalized linear models, Third edition. SAGE, Los Angeles
Geiger R (1950) The climate near the ground, 2nd edn. Harvard University Press, Cambridge, MA
Gill NS, Turner MG, Brown CD et al (2022) Limitations to propagule dispersal will constrain postfire recovery of plants and fungi in western coniferous forests. Bioscience 72:347–364.
Grimm V, Revilla E, Berger U et al (2005) Pattern-oriented modeling of agent-based complex systems: Lessons from ecology. Science 310:987–991.
Gustafson EJ (2013) When relationships estimated in the past cannot be used to predict the future: Using mechanistic models to predict landscape ecological dynamics in a changing world. Landsc Ecol 28:1429–1437.
Hannah L, Flint L, Syphard AD et al (2014) Fine-grain modeling of species' response to climate change: holdouts, stepping-stones, and microrefugia. Trends Ecol Evol 29:390–397.
Hansen WD, Braziunas KH, Rammer W et al (2018) It takes a few to tango: Changing climate and fire regimes can cause regeneration failure of two subalpine conifers. Ecology 99:966–977.
Harmon ME, Bond-Lamberty B, Tang J, Vargas R (2011) Heterotrophic respiration in disturbed forests: A review with examples from North America. Journal of Geophysical Research Biogeosciences. 116: G00K04.
Hoecker TJ, Hansen WD, Turner MG (2020) Topographic position amplifies consequences of short-interval stand-replacing fires on postfire tree establishment in subalpine conifer forests. Forest Ecol Manag 478:118523.
Jenerette GD, Anderson KE, Cadenasso ML et al (2022) An expanded framework for wildland–urban interfaces and their management. Front Ecol Environ 20:516–523.
Kätterer T, Andrén O (2001) The ICBM family of analytically solved models of soil carbon, nitrogen and microbial biomass dynamics — descriptions and application examples. Ecol Model 136:191–207.
Lenoir J, Hattab T, Pierre G (2017) Climatic microrefugia under anthropogenic climate change: implications for species redistribution. Ecography 40:253–266.
Maclean IMD, Klinges DH (2021) Microclimc: A mechanistic model of above, below and within-canopy microclimate. Ecol Model 451:109567.
Maroschek M, Seidl R, Poschlod B, Senf C (2023) Quantifying patch size distributions of forest disturbances in protected areas across the European Alps. J Biogeogr 51:368–381.
Meeussen C, Govaert S, Vanneste T et al (2021) Microclimatic edge-to-interior gradients of European deciduous forests. Agric for Meteorol 311:108699.
Menge JH, Magdon P, Wöllauer S, Ehbrecht M (2023) Impacts of forest management on stand and landscape-level microclimate heterogeneity of European beech forests. Landsc Ecol 38:903–917.
Mina M, Messier C, Duveneck MJ et al (2022) Managing for the unexpected: Building resilient forest landscapes to cope with global change. Glob Change Biol 28:4323–4341.
Nitschke CR, Innes JL (2008) A tree and climate assessment tool for modelling ecosystem response to climate change. Ecol Model 210:263–277.

Pastore MA, Classen AT, D'Amato AW et al (2022) Cold-air pools as microrefugia for ecosystem functions in the face of climate change. Ecology 103:e3717.
Peters DPC, Bestelmeyer BT, Turner MG (2007) Cross-scale interactions and changing pattern-process relationships: Consequences for system dynamics. Ecosystems 10:790–796.
Rammer W, Thom D, Baumann M et al (2024) The individual-based forest landscape and disturbance model iLand: Overview, progress, and outlook. Ecol Model 495:110785.
Reiner R, Zedrosser A, Zeiler H et al (2021) Forests buffer the climate-induced decline of body mass in a mountain herbivore. Global Change Biol 27:3741–3752.
Rothermel RC (1983) How to predict the spread and intensity of forest and range fires. USDA Forest Service, Ogden, UT
Sanczuk P, De Pauw K, De Lombaerde E et al (2023) Microclimate and forest density drive plant population dynamics under climate change. Nat Clim Chang 13:840–847.
Seidl R, Rammer W (2017) Climate change amplifies the interactions between wind and bark beetle disturbances in forest landscapes. Landsc Ecol 32:1485–1498.
Seidl R, Rammer W, Scheller RM, Spies TA (2012a) An individual-based process model to simulate landscape-scale forest ecosystem dynamics. Ecol Model 231:87–100.
Seidl R, Spies TA, Rammer W et al (2012b) Multi-scale drivers of spatial variation in old-growth forest carbon density disentangled with Lidar and an individual-based landscape model. Ecosystems 15:1321–1335.
Seidl R, Rammer W, Blennow K (2014) Simulating wind disturbance impacts on forest landscapes: Tree-level heterogeneity matters. Environ Model Softw 51:1–11.
Seidl R, Rammer W (2024) iLand online model documentation. https://iland-model.org/. Accessed 7 Feb 2023
Senf C, Pflugmacher D, Hostert P, Seidl R (2017) Using Landsat time series for characterizing forest disturbance dynamics in the coupled human and natural systems of Central Europe. ISPRS J Photogramm Remote Sens 130:453–463.
Storck P, Lettenmaier DP, Bolton SM (2002) Measurement of snow interception and canopy effects on snow accumulation and melt in a mountainous maritime climate, Oregon United States. Water Resour Res 38:1223.
Stritih A, Senf C, Seidl R et al (2021) The impact of land-use legacies and recent management on natural disturbance susceptibility in mountain forests. For Ecol Manag 484:118950.
Thom D, Sommerfeld A, Sebald J et al (2020) Effects of disturbance patterns and deadwood on the microclimate in European beech forests. Agric for Meteorol 291:108066.
Thom D, Rammer W, Laux P et al (2022) Will forest dynamics continue to accelerate throughout the 21st century in the Northern Alps? Global Change Biol 28:3260–3274.
Turner MG (2010) Disturbance and landscape dynamics in a changing world. Ecology 91:2833–2849.
Vandewiele M, Geres L, Lotz A et al (2023) Mapping spatial microclimate patterns in mountain forests from LiDAR. Agric for Meteorol 341:109662.
Vanwalleghem T, Meentemeyer RK (2009) Predicting forest microclimate in heterogeneous landscapes. Ecosystems 12:1158–1172.
von Arx G, Pannatier EG, Thimonier A, Rebetez M (2013) Microclimate in forests with varying leaf area index and soil moisture: Potential implications for seedling establishment in a changing climate. J Ecol 101:1201–1213.
White JW, Rassweiler A, Samhouri JF et al (2014) Ecologists should not use statistical significance tests to interpret simulation model results. Oikos 123:385–388.
Wiens JA (1989) Spatial scaling in ecology. Funct Ecol 3:385–397.
Wolf KD, Higuera PE, Davis KT, Dobrowski SZ (2021) Wildfire impacts on forest microclimate vary with biophysical context. Ecosphere 12:e03467.
Xu C, De Frenne P, Blondeel H et al (2023) Light more than warming impacts understory tree seedling growth in a temperate deciduous forest. For Ecol Manag 549:121496.
Zellweger F, Coomes D, Lenoir J et al (2019) Seasonal drivers of understorey temperature buffering in temperate deciduous forests across Europe. Global Ecol Biogeogr 28:1774–1786.
Zellweger F, de Frenne P, Lenoir J et al (2020) Forest microclimate dynamics drive plant responses to warming. Science 368:772–775.

Microclimate temperature effects propagate across scales in forest ecosystems

Kristin H. Braziunas, Werner Rammer, Pieter De Frenne, Joan Díaz-Calafat, Per-Ola Hedwall, Cornelius Senf, Dominik Thom, Florian Zellweger, and Rupert Seidl

Supplementary materials and methods

Empirical temperature offset models

Within each forested study site, daily minimum and maximum microclimate temperature were recorded at plot centers either with Lascar Easy Log EL-USB-1 at 1 m height (Zellweger et al. 2019; Meeussen et al. 2021) or HOBO Pendant MX Water Temperature loggers at 1.2 m height (Díaz-Calafat et al. 2023). Prior to model fitting, temperature data were reviewed and cleaned to identify and remove snow days, erroneous time periods, and extreme outliers. This removed 5% of daily data from further analysis.

Snow days. We identified days when temperature loggers were covered with snow as days where the daily temperature range was < 1°C, the average maximum daily temperature was < 1°C in a 9-day moving window, and the average daily temperature range was < 2°C within the same 9-day moving window (Aalto et al. 2022; Tyystjärvi et al. 2023). Since loggers were at 1-1.2 m height, this only occurred in some winters in plots in Scandinavia. Subsequently, all days within a 5-day moving window were classified as snow days if at least one day was snow-covered (Tyystjärvi et al. 2023).

Erroneous time periods. Microclimate loggers were grouped by region to identify erroneous time periods. Anomalies were automatically detected by taking the 30-day running mean of maximum and minimum temperature for all loggers in a region and then identifying measurements that were more than three standard deviations from the mean value (*sensu* Aalto et al. 2022). We then visually evaluated all loggers with anomalies by comparing time series with other loggers in the same region and, when applicable, at the same site within a region (*sensu* Meeussen et al. 2021). If loggers exhibited sustained time periods with anomalous values, did not align with other loggers at the same region or site, or did not exhibit expected seasonal trends, these time periods were classified as erroneous (e.g., potentially a period when the logger was uprooted or damaged) and removed from analyses.

Extreme outliers. Individual outlier values were removed based on similar criteria. Extreme outliers were identified as any values that was greater than three standard deviations from the 30-day running mean for each logger and as values that were < -50°C or > 50°C (Tyystjärvi et al. 2023). These outliers were also removed from analyses.

Predictor variables. Predictor variable selection was based on important predictors identified in previous studies and *a priori* expectations based on ecological relationships (Table 2 in main manuscript). Other predictors were considered but excluded due to high collinearity (e.g., phenology with macroclimate temperature) or duplicative information (e.g., elevation with macroclimate temperature, cold air drainage with topographic position index), unbalanced representation among the different studies (e.g., proportion deciduous or coniferous), lack of variability within the study landscape (e.g., distance to coast does not vary meaningfully within Berchtesgaden), and inadequate coverage of values in the study landscape (e.g., relatively shallower stopes in microclimate dataset and steeper slopes in Berchtesgaden). Final predictors were not strongly correlated (all bivariate Pearson's $r < 0.5$) and summary statistics by study area are included in Table S1.

Table S1. Summary data on microclimate and macroclimate temperature data collection dates and mean, standard deviation, and range of dependent and predictor variables used in empirical temperature offset models for each of the three studies and for all studies combined.

Variable	Units	**Díaz-Calafat et al. 2023** mean (sd) min-max	**Meeussen et al. 2021** mean (sd) min-max	**Zellweger et al. 2019** mean (sd) min-max	**All studies** mean (sd) min-max
Data collection					
Date range	–	Jan 2020-July 2021	June 2018-May 2020	Mar 2017-Jan 2018	2017-2021
Number of observations (monthly averages of daily values)	–	2381	4370	1004	7755
Dependent variables					
Average daily minimum microclimate temperature offset ($Tmin_{offset}$)	°C	-0.03 (1.3) -2.5-3.4	1.28 (1.59) -3.9-8.26	0.89 (1.1) -1.97-4.11	0.83 (1.56) -3.9-8.26
Average daily maximum microclimate temperature offset ($Tmax_{offset}$)	°C	0.54 (1.49) -2.88-8.78	-5.02 (4.23) -18.25-14.23	-0.83 (1.4) -4.34-3.98	-2.77 (4.21) -18.25-14.23
Predictor variables					
Average daily minimum macroclimate temperature ($Tmin_{macroclimate}$)	°C	3.26 (6.23) -12.44-15.42	5.09 (5.34) -7.5-16.5	6.28 (4.69) -5.58-13.88	4.68 (5.64) -12.44-16.5
Average daily maximum macroclimate temperature ($Tmax_{macroclimate}$)	°C	11.48 (7.55) -5.37-24.96	22.54 (10.66) -0.52-44.93	14.83 (6.83) 0.89-28.07	18.15 (10.65) -5.37-44.93
Northness	dim[-1,1]	-0.22 (0.69) -1-1	-0.47 (0.67) -1-1	-0.11 (0.73) -1-1	-0.35 (0.7) -1-1
Topographic position index (TPI)	m	-0.02 (4.45) -8.71-12.33	-3.33 (24.71) -105.43-63.2	4.94 (13.68) -15.98-66.8	-1.24 (19.55) -105.43-66.8
Leaf area index (LAI)	$m^2 m^{-2}$	2.65 (1.33) 0.37-6.33	2.53 (1.35) 0.3-7.74	3.39 (1.54) 0.52-9.44	2.67 (1.4) 0.3-9.44
Shade tolerance (STol)	dim[1,5]	2.53 (0.71) 1-3.5	3.07 (0.88) 1.06-5	3.68 (0.68) 2-5	2.98 (0.88) 1-5

Daily minimum and maximum macroclimate temperature for each site was recorded from either nearby weather stations (Zellweger et al. 2019; Díaz-Calafat et al. 2023) or from an identical temperature logger installed nearby in open conditions (Meeussen et al. 2021). Macroclimate loggers installed in open conditions were also quality checked, and snow days and extreme outliers were identified and excluded as described above. Temperature offset was then calculated as microclimate minus macroclimate temperature for daily minimum and maximum values (Equations S1-S2).

$$Tmin_{offset} = Tmin_{microclimate} - Tmin_{macroclimate} \quad \text{(Eq. S1)}$$

$$Tmax_{offset} = Tmax_{microclimate} - Tmax_{macroclimate} \quad \text{(Eq. S2)}$$

Negative offset values indicate that microclimate temperatures are cooler underneath the forest canopy relative to macroclimate temperatures, whereas positive values indicate subcanopy temperatures are warmer. Daily temperature offsets were averaged for each month, and only months with at least 15 daily observations were included in model fitting.

Topographic predictors were derived from field plot coordinates and a 25 m resolution digital elevation model (EU-DEM 2016). Forest structure and composition predictors were calculated from forest inventory data including individual tree species and diameter at breast height (DBH) for all trees with DBH > 7.5 cm in a 9 m radius plot centered on the location of the microclimate logger. We quantified plot-level variables using previously compiled and tested species-specific trait values for foliage biomass allometry, specific leaf area, and shade tolerance for Central European tree species simulated in iLand (Seidl et al. 2012; Thom et al. 2017, 2022). Species not present in this dataset were assigned biomass allometrics from a morphologically similar species (based on Falster et al. 2015; Forrester et al. 2017). Additional data on shade tolerance was procured from Niinemets & Valladares (2006) via the TRY Plant Trait Database (Kattge et al. 2020).

A random intercept effect for study (n = 3) was included to account for variance due to methodological or other differences among studies (e.g., different microclimate temperature sensors, macroclimate data sources, measurement height, and data cleaning processes) not explained by fixed effects. This assumed that study was independent of the fixed effects. We evaluated this assumption by testing for multicollinearity among all predictors using generalized variance inflation factors (GVIF), which when rescaled based on degrees of freedom are suitable for evaluating correlation strength for categorical predictors with more than two levels (Fox and Monette 1992; Fox 2016). The squared scaled GVIF is identical to the variance inflation factor for continuous variables and interpreted using the same ranges of values to assess correlation strength. We further evaluated the inclusion of study by comparing residual boxplots between models with or without study as a predictor; the inclusion of study as a random effect removed directional trends in median residual values, although some unequal variance remained (Figure S1).

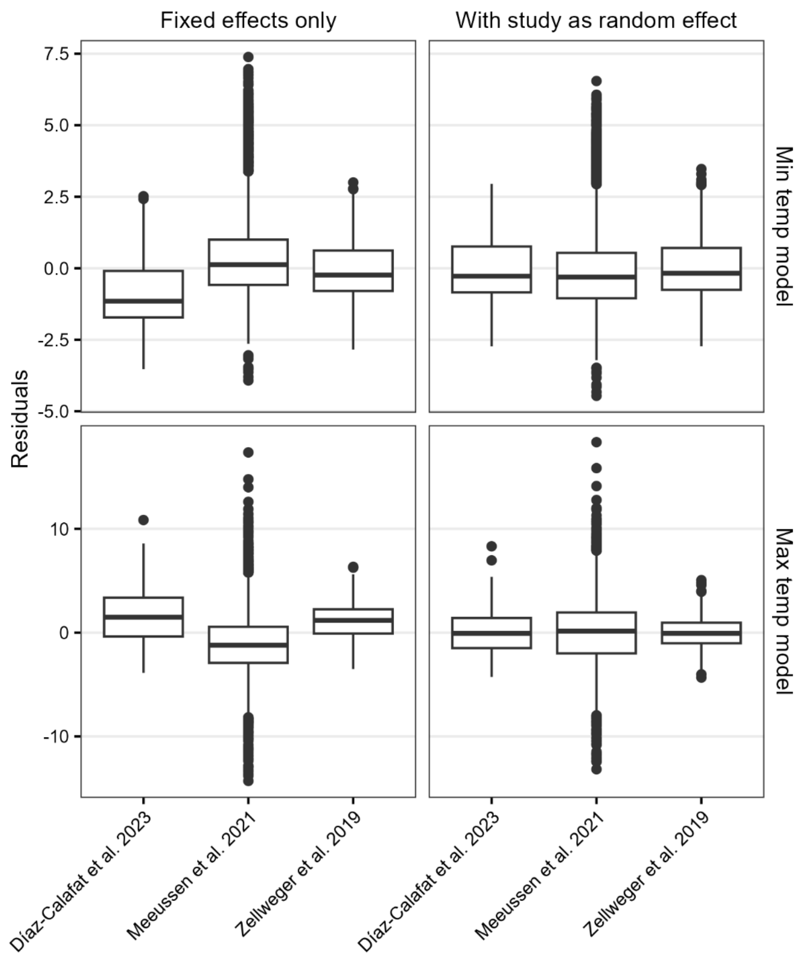

Figure S1. Boxplots showing trends and variability in residual values among different studies for linear models with only fixed effects (study not included as a predictor; left column) and for linear mixed effects models when study was included as a random intercept effect (right column). Top row: minimum temperature offset model, Bottom row: maximum temperature offset model.

Model diagnostics and decision-making. Linear mixed effects model diagnostics based on residual and quantile-quantile plots showed slight deviations from assumptions of normality, linearity, and equal variance (Figures S2-S3). We used and considered multiple approaches for improving model assumptions, including removing erroneous values and outliers (described above), using the monthly average of daily minimum and maximum temperatures rather than the daily values, adding more predictors, transforming predictors, including or excluding study as a random effect, and fitting separate models for each study. Adding new or transforming predictors did not improve assumptions, but using the monthly average of daily values and including study as a random effect did improve assumptions (e.g., see Figure S1 above). Separate models fit to each study showed that assumption violations varied by dependent variable and by study (Figures S4-S5).

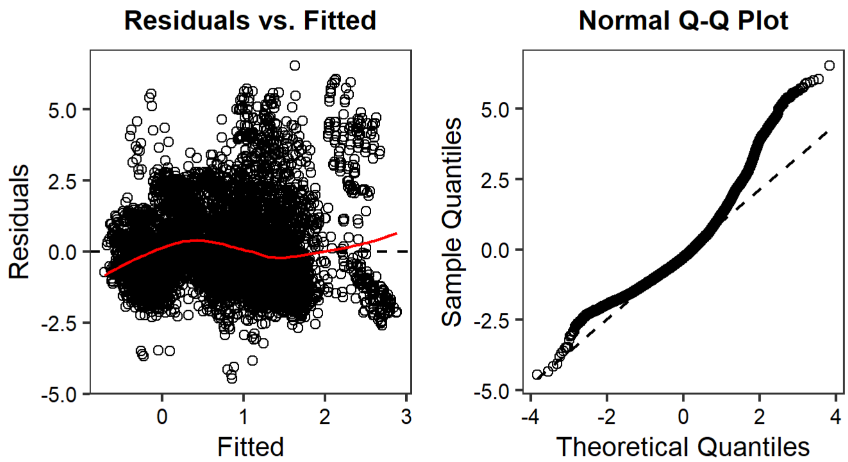

Figure S2. Final linear mixed effects model diagnostics, including residuals versus fitted values and quantile-quantile plot, for minimum temperature offset.

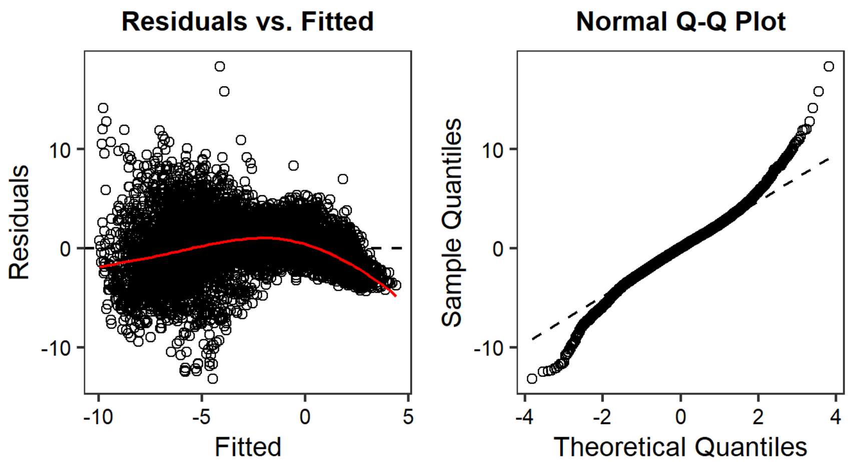

Figure S3. Final linear mixed effects model diagnostics, including residuals versus fitted values and quantile-quantile plot, for maximum temperature offset.

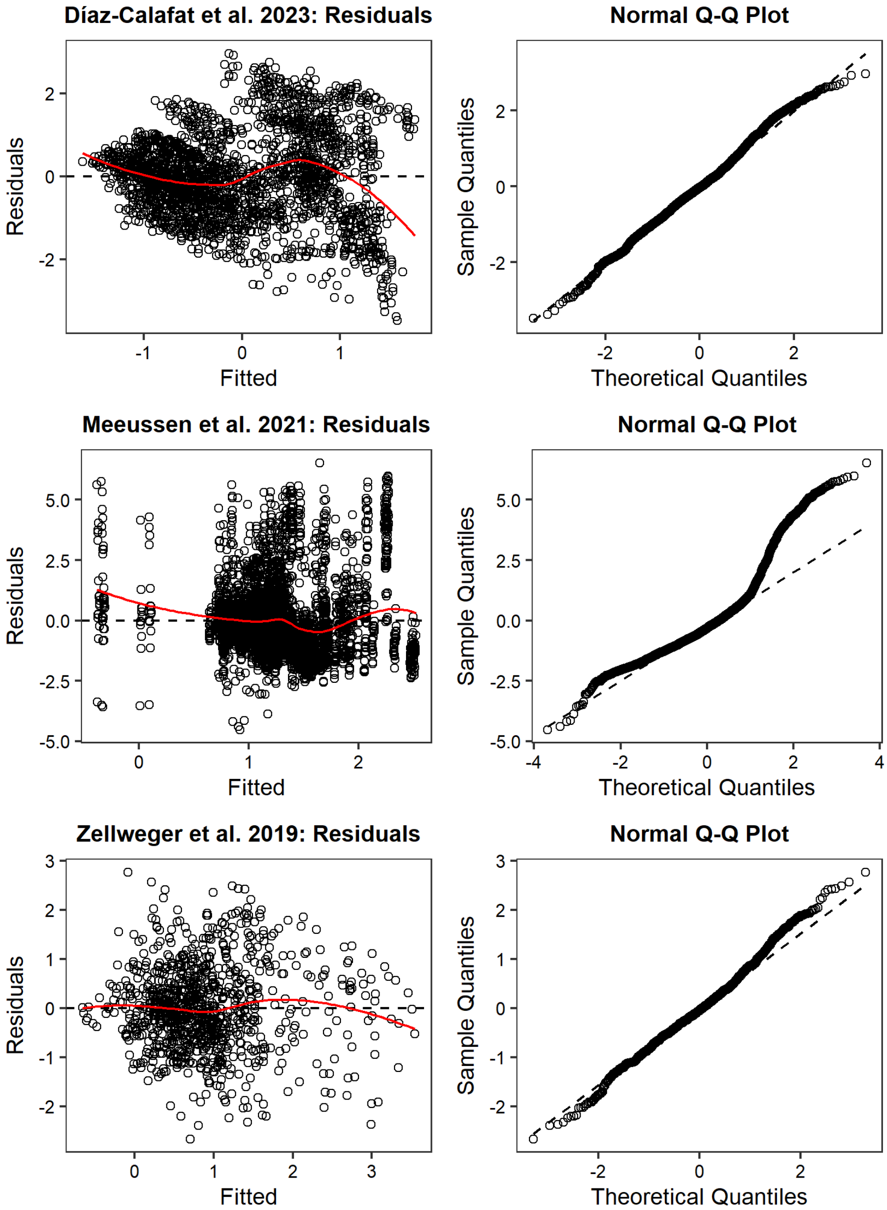

Figure S4. Linear model diagnostics, including residuals versus fitted values (left column) and quantile-quantile plots (right column), for minimum temperature offset models fit to each study separately (rows).

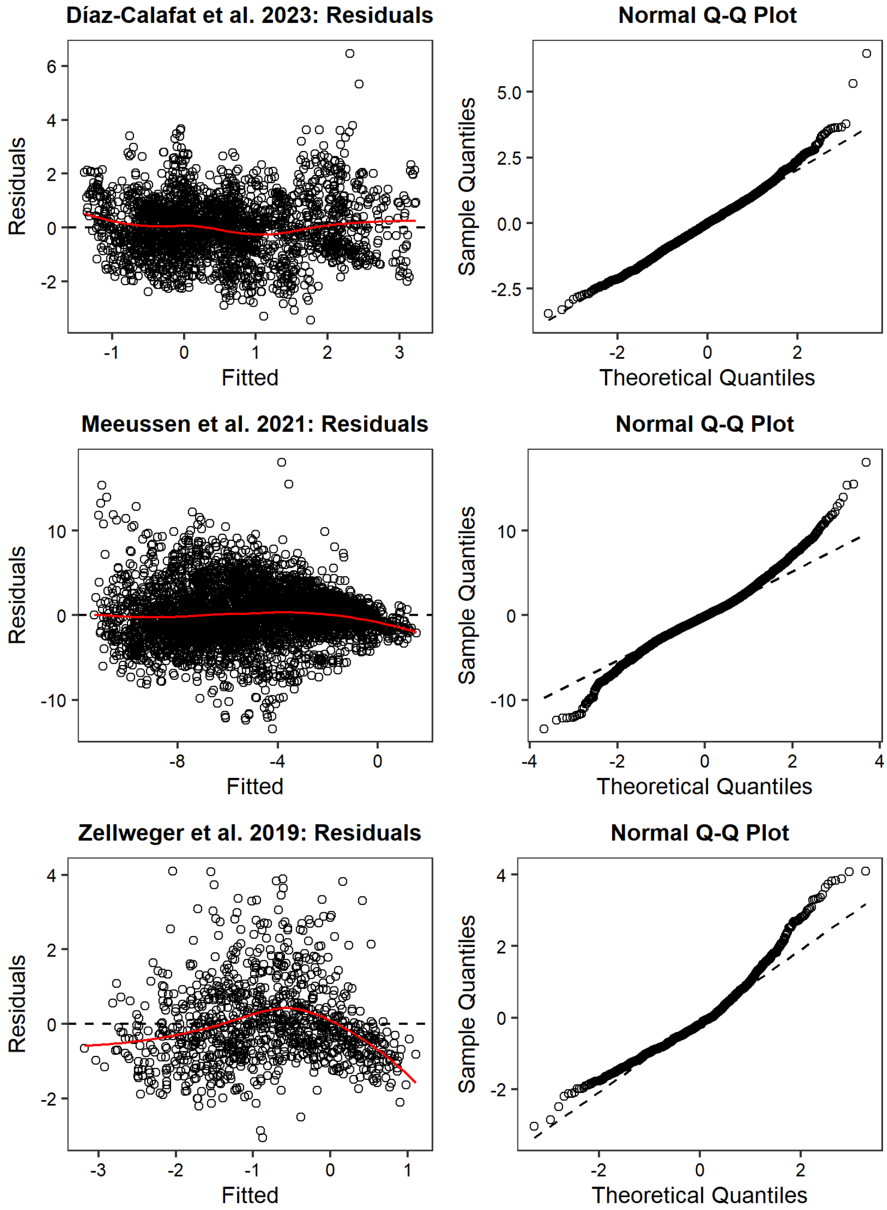

Figure S5. Linear model diagnostics, including residuals versus fitted values (left column) and quantile-quantile plots (right column), for maximum temperature offset models fit to each study separately (rows).

We considered model goals and the balance of generality, realism, and precision in final model decision-making (Levins 1966). For the purposes of implementing microclimate temperature offsets in a process-based forest landscape simulation model, we prioritized simplicity, generality, and ecological realism at the expense of additional model precision in the fit of the statistical model. Thus, we chose a linear model for simplicity and included all data despite assumption violations to improve generality. We further considered ecological realism in model evaluations, such as expectations from the literature and biophysical principles for relationships between fixed effects and predicted offsets, seasonal and forest type variation in predicted offsets, and comparisons with independent data. Finally, we considered and took steps to constrain the potential range of predicted values. Predictions tended to be more conservative relative to observations (i.e., overpredicted at low extremes and underpredicted at high extremes; Figure S6a-b). We truncated all predictor values to the maximum and minimum values used in model fitting to avoid extrapolating beyond the range of values used to train the models.

Final models. Final linear mixed effects models predicting the monthly average of daily minimum ($R^2_c = 0.24$, $R^2_m = 0.07$) and maximum ($R^2_c = 0.47$, $R^2_m = 0.29$) temperature offsets were fit to n = 7,755 observations in n = 497 plots (Equations S3-S4; Tables 3-4; Figure S6). Note that Equations show fixed effects and the average intercept across studies; the random effect (study) would be reflected by having a different intercept for each study.

$$Tmin_{offset} = 1.4570 - 0.0248 \times Tmin_{macroclimate} + 0.2627 \times Northness + 0.0158 \times TPI + 0.0227 \times LAI - 0.2031 \times STol \quad \text{(Eq. S3)}$$

$$Tmax_{offset} = 0.9767 - 0.1932 \times Tmax_{macroclimate} - 0.5729 \times Northness + 0.0140 \times TPI - 0.3948 \times LAI + 0.4419 \times STol \quad \text{(Eq. S4)}$$

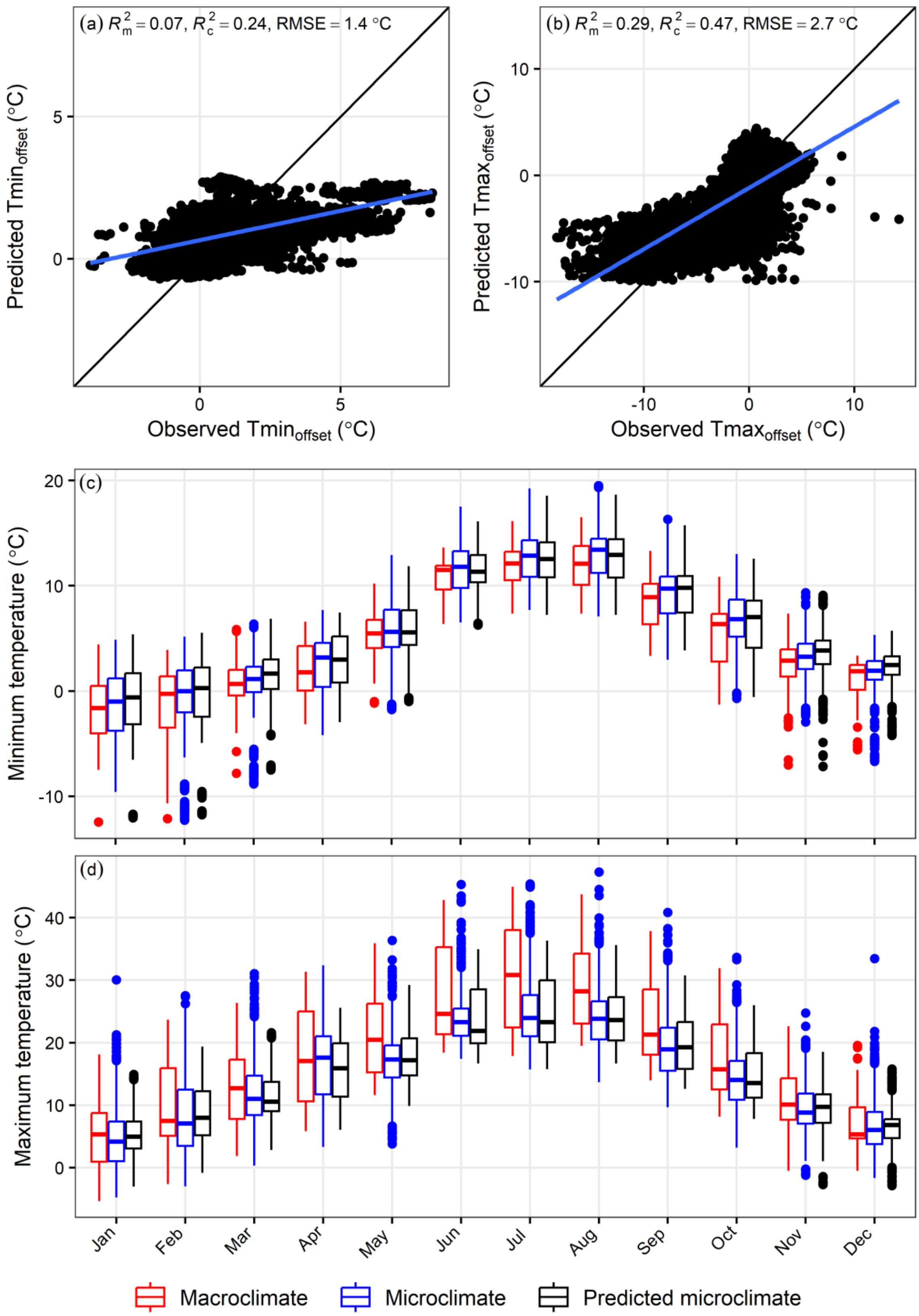

Figure S6. (a-b) Predicted versus observed average daily minimum (a) and maximum (b) microclimate temperature offset from linear mixed effects models fit to monthly averages (n = 7,755 observations from three studies). Black line is 1:1 line, blue line is linear fit. (c-d) Temporal variability in macroclimate, microclimate, and predicted microclimate for average daily minimum (c) and maximum (d) temperature.

Initial conditions for iLand simulations

Initial forest structure and species composition was mapped from 3,559 regularly spaced forest inventory plots and a forest type map. Daily climate (1980-2009) was derived from bias corrected dynamic regional climate projections (Warscher et al. 2019) using 35 local weather stations and statistically downscaled to 100 m resolution accounting for the effect of elevation. Historical wind event speed, direction, and day of year were modeled from regional meteorological station measurements, and simulated wind and bark beetle disturbances aligned well with past observations (Thom et al. 2022). Soil texture and fertility were mapped from regional data (Konnert 2004), and topographic variables were derived from a digital elevation model (EU-DEM 2016) downscaled from 25 to 10 m resolution using bilinear interpolation.

Analyses across scales

At local scales, we compared microclimate temperature effects on forest processes in dense forested stands, defined as having overstory LAI > 4 m^2 m^{-2} (von Arx et al. 2013). Using the first 30 years per simulation replicate, we computed the annual mean value for indicators of each of the three focal processes: heterotrophic respiration (Mg C ha^{-1}) as an indicator of decomposition, number of completed beetle generations as an indicator of bark beetle development rates, and tree regeneration density (total and species-specific stems ha^{-1} for stems < 4 m height) as an indicator of tree establishment.

At mesoscales, we evaluated disturbance effects on the same decomposition, bark beetle, and establishment indicators as the post- minus pre-disturbance mean value for each disturbance patch in microclimate and macroclimate simulations. Stands were considered disturbed if at least half of the 1-ha area experienced a bark beetle or windthrow event over the first 10 simulation years, to account for multi-year bark beetle spread or wind-beetle interactions. Patches (minimum size = 1 ha) were then classified using the 8-neighbor rule. Pre-disturbance indicators were calculated for simulation year 0 and post-disturbance for year

15 (i.e., 5-15 years since disturbance) based on forest recovery rates and the timing of peak microclimate temperature buffering in this landscape (Vandewiele et al. 2023).

Mesoscale differences in tree regeneration were also evaluated for six representative species that varied in elevational range and temperature sensitivity. These included beech and silver fir [submontane-montane zone, warm-preferring with Ellenberg Indicator Value (EIV) for temperature = 5; Ellenberg & Leuschner, 2010], spruce and Swiss stone pine (subalpine, cold-preferring with EIV = 3 and 2, respectively), and sycamore maple (*Acer pseudoplatanus* L.) and larch (montane and subalpine, respectively, temperature indifferent). The elevational regeneration range for each species was represented with 100 m bands centered on the approximate lower bound, median, and upper bound of its elevational regeneration distribution in the Bavarian Alps (Ewald 2012). Lower bounds were excluded from analysis if they fell below the minimum elevation in the Berchtesgaden landscape (~600 m). Variable effects of microclimate along the elevational regeneration range were quantified as the relative difference in stem density between microclimate and macroclimate simulations for each species and elevation band, averaged across the first 30 simulation years.

At the landscape scale, we compared cumulative net ecosystem productivity (NEP), total carbon, carbon pools, cumulative disturbance mortality, and tree species composition (trees > 4 m height) based on basal area after 1,000 years of forest development with or without microclimate temperature buffering. Indicators that were not cumulative (carbon pools and species basal area) were averaged over the last 30 simulation years. We also compared relative differences in landscape scale indicators between the first and last 30 simulation years (here, annual rather than cumulative values were used for NEP and disturbance) and with the local scale indicators described above to evaluate how microclimate effects changed over time and across scales.

Sensitivity analysis

A sensitivity analysis was performed to determine which process most strongly contributed to landscape scale change in cumulative NEP, total carbon, and individual carbon pools when driven by microclimate rather than macroclimate temperature. To determine relative effects, microclimate temperature buffering was turned “on” or “off” for each of the three processes (decomposition, bark beetle development, tree establishment), and simulations were run for all combinations (n = 10 replicates of each 2^3 processes = 80 total replicates). For each replicate, forest development was simulated for 30 years under historical climate, random sequences of wind events, and dynamic bark beetle disturbances starting from contemporary forest conditions in Berchtesgaden National Park. Cumulative NEP at year 30 and average carbon pools were normalized by subtracting the corresponding macroclimate replicate (microclimate = “off” for all processes) and dividing by the range of simulation means (i.e., the range of all eight process combinations after averaging across the 10 replicates, so that mean differences will be within +/-1).

Cumulative NEP, total carbon, and all carbon pools except live C were most sensitive to microclimate temperature buffering effects on decomposition (Figure S7). Dampened bark beetle development rates due to microclimate buffering resulted in the greatest increases in live C and decreases in dead woody C that partially offset gains from reduced decomposition.

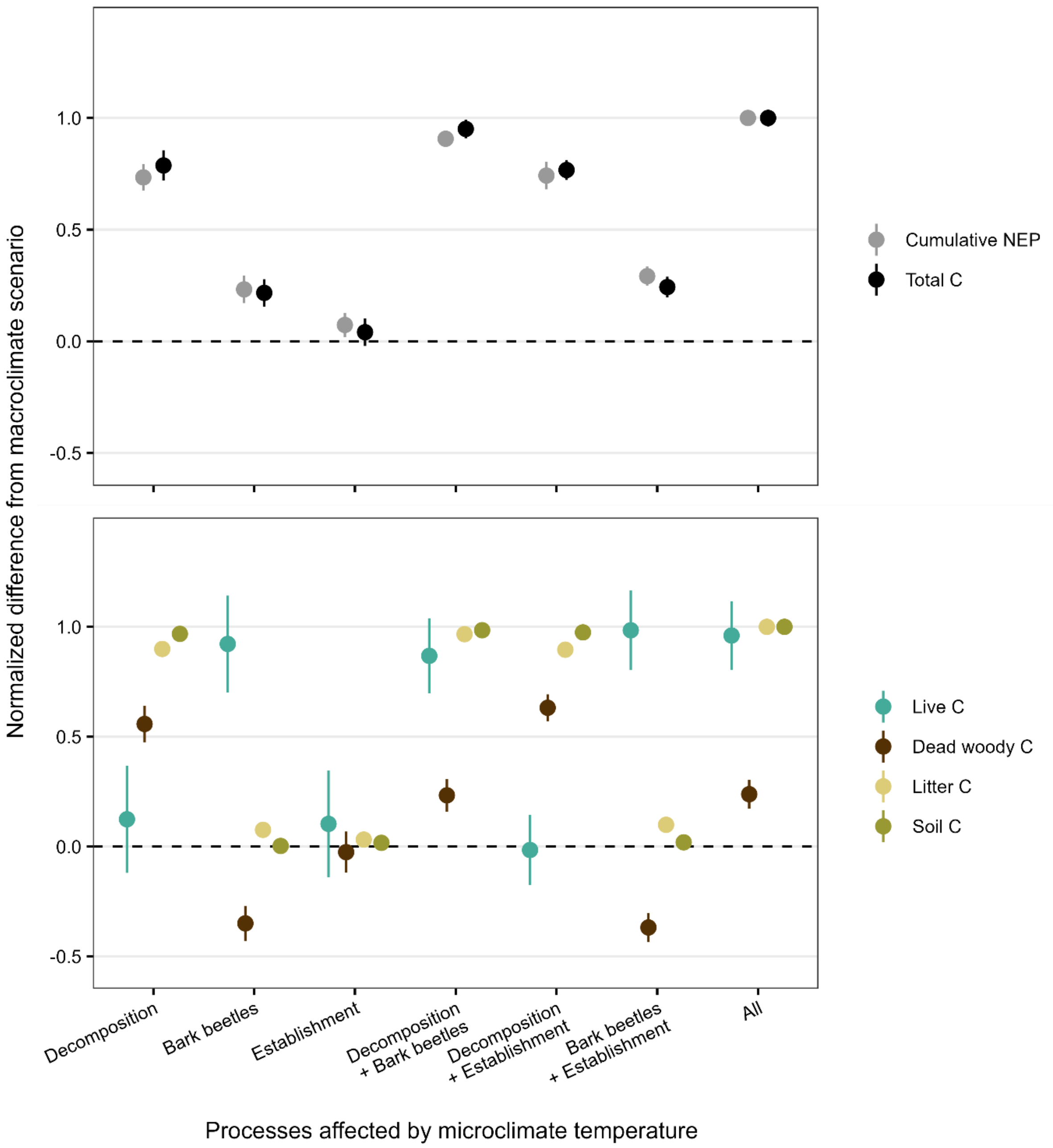

Figure S7. Sensitivity analysis showing the effect of driving simulations with microclimate instead of macroclimate for all combinations of three forest processes on (a) cumulative net ecosystem productivity (NEP) and total carbon (C) or (b) different carbon pools. X axis shows which processes are driven by microclimate. Points and ranges are derived from $n = 10$ replicates of each and show the mean change (point) and two standard errors (range). All values have been normalized by subtracting the corresponding macroclimate replicate value and dividing by the range of simulation means [i.e., the range of all eight process combinations after averaging across the 10 replicates, so that mean differences (points) will be within +/-1].

Software

All statistical analyses were performed and, with the exception of Figure 1, all figures were created using R (R Core Team 2024) version 4.3.2. We specifically used the packages car (Fox and Weisberg 2019), corrplot (Wei and Simko 2021), cowplot (Wilke 2020), ggnewscale (Campitelli 2023), ggpubr (Kassambara 2023), landscapemetrics (Hesselbarth et al. 2019), lme4 (Bates et al. 2015), lmerTest (Kuznetsova et al. 2017), lubridate (Grolemund and Wickham 2011), ModelMetrics (Hunt 2020), MuMIn (Bartoń 2023), openxlsx (Schauberger and Walker 2023), plotrix (Lemon 2006), RSQLite (Müller et al. 2023), sf (Pebesma 2018; Pebesma and Bivand 2023), terra (Hijmans 2023), tidyverse (Wickham et al. 2019), and zoo (Zeileis and Grothendieck 2005). Figure color schemes were derived from Color Brewer 2.0 (Brewer and Harrower 2013), khroma (Frerebeau 2023), and Paul Tol's Color Schemes (Tol 2023).

References

Aalto J, Tyystjärvi V, Niittynen P, et al (2022) Microclimate temperature variations from boreal forests to the tundra. Agricultural and Forest Meteorology 323:109037. https://doi.org/10.1016/j.agrformet.2022.109037

Bartoń K (2023) MuMIn: Multi-model inference. R package version 1.47.5. https://CRAN.R-project.org/package=MuMIn

Bates D, Mächler M, Bolker BM, Walker SC (2015) Fitting linear mixed-effects models using lme4. Journal of Statistical Software 67:1–48. https://doi.org/10.18637/jss.v067.i01

Brewer C, Harrower M (2013) Color Brewer 2.0: Color advice for cartography. https://colorbrewer2.org/. Accessed 31 Jan 2024

Campitelli E (2023) ggnewscale: Multiple fill and colour scales in ggplot2. R package version 0.4.9. https://CRAN.R-project.org/package=ggnewscale

Díaz-Calafat J, Uria-Diez J, Brunet J, et al (2023) From broadleaves to conifers: The effect of tree composition and density on understory microclimate across latitudes. Agricultural and Forest Meteorology 341:109684. https://doi.org/10.1016/j.agrformet.2023.109684

Ellenberg H, Leuschner C (2010) Vegetation Mitteleuropas mit den Alpen. In ökologischer, dynamischer und historischer Sicht, 6th edn. UTB, Stuttgart

EU-DEM (2016) European Digital Elevation Model (EU-DEM), version 1.1. http://land.copernicus.eu/pan-european/satellite-derived-products/eu-dem/eu-dem-v1.1/view. Accessed 31 Jul 2023

Ewald J (2012) Vegetation databases provide a close-up on altitudinal tree species distribution in the Bavarian Alps. Vegetation databases for the 21st century–Biodiversity & Ecology 4:41–48

Falster DS, Duursma RA, Ishihara MI, et al (2015) BAAD: a Biomass And Allometry Database for woody plants. Ecology 96:1445–1445. https://doi.org/10.1890/14-1889.1

Forrester DI, Tachauer IHH, Annighoefer P, et al (2017) Generalized biomass and leaf area allometric equations for European tree species incorporating stand structure, tree age and climate. Forest Ecology and Management 396:160–175. https://doi.org/10.1016/j.foreco.2017.04.011

Fox J (2016) Applied regression analysis and generalized linear models, Third edition. SAGE, Los Angeles

Fox J, Monette G (1992) Generalized collinearity diagnostics. Journal of the American Statistical Association 87:178–183. https://doi.org/10.1080/01621459.1992.10475190

Fox J, Weisberg S (2019) An R companion to applied regression. Sage, Thousand Oaks, CA

Frerebeau N (2023) khroma: Colour schemes for scientific data visualization. R package version 1.11.0. https://packages.tesselle.org/khroma

Grolemund G, Wickham H (2011) Dates and times made easy with lubridate. Journal of Statistical Software 40:1–25. https://doi.org/10.18637/jss.v040.i03

Hesselbarth MHK, Sciaini M, With KA, et al (2019) landscapemetrics: An open-source R tool to calculate landscape metrics. Ecography 42:1648–1657. https://doi.org/10.1111/ecog.04617

Hijmans RJ (2023) terra: Spatial data analysis. R package version 1.7-55. https://CRAN.R-project.org/package=terra

Hunt T (2020) ModelMetrics: Rapid calculation of model metrics. R package version 1.2.2.2. https://CRAN.R-project.org/package=ModelMetrics

Kassambara A (2023) ggpubr: ggplot2 based publication ready plots. R package version 0.6.0. https://CRAN.R-project.org/package=ggpubr

Kattge J, Bönisch G, Díaz S, et al (2020) TRY plant trait database – enhanced coverage and open access. Global Change Biology 26:119–188. https://doi.org/10.1111/gcb.14904

Konnert V (2004) Standortkarte Nationalpark Berchtesgaden. Nationalpark Berchtesgaden, Forschungsbericht 49, Berchtesgaden, DE

Kuznetsova A, Brockhoff PB, Christensen RHB (2017) lmerTest Package: Tests in Linear Mixed Effects Models. Journal of Statistical Software 82:1–26. https://doi.org/10.18637/jss.v082.i13

Lemon J (2006) Plotrix: A package in the red light district of R. R-News 6:8–12

Levins R (1966) The strategy of model building in population biology. American Scientist 54:421–431

Meeussen C, Govaert S, Vanneste T, et al (2021) Microclimatic edge-to-interior gradients of European deciduous forests. Agricultural and Forest Meteorology 311:108699. https://doi.org/10.1016/j.agrformet.2021.108699

Müller K, Wickham H, James DA, Falcon S (2023) RSQLite: "SQLite" interface for R. R package version 2.3.3. https://CRAN.R-project.org/package=RSQLite

Niinemets Ü, Valladares F (2006) Tolerance to shade, drought, and waterlogging of temperate northern hemisphere trees and shrubs. Ecological Monographs 76:521–547. https://doi.org/10.1890/0012-9615(2006)076[0521:TTSDAW]2.0.CO;2

Pebesma E (2018) Simple features for R: Standardized support for spatial vector data. R Journal 10:439–446. https://doi.org/10.32614/rj-2018-009

Pebesma E, Bivand R (2023) Spatial Data Science: With Applications in R., 1st Edition. Chapman and Hall/CRC, Boca Raton, FL

R Core Team (2024) R: A language and environment for statistical computing. Vienna, Austria

Schauberger P, Walker A (2023) openxlsx: Read, write and edit xlsx files. R package version 4.2.5.2. https://CRAN.R-project.org/package=openxlsx

Seidl R, Rammer W, Scheller RM, Spies TA (2012) An individual-based process model to simulate landscape-scale forest ecosystem dynamics. Ecological Modelling 231:87–100. https://doi.org/10.1016/j.ecolmodel.2012.02.015

Thom D, Rammer W, Dirnböck T, et al (2017) The impacts of climate change and disturbance on spatio-temporal trajectories of biodiversity in a temperate forest landscape. Journal of Applied Ecology 54:28–38. https://doi.org/10.1111/1365-2664.12644

Thom D, Rammer W, Laux P, et al (2022) Will forest dynamics continue to accelerate throughout the 21st century in the Northern Alps? Global Change Biology 28:3260–3274. https://doi.org/10.1111/gcb.16133

Tol P (2023) Paul Tol's Notes: Colour schemes and templates. https://personal.sron.nl/~pault/. Accessed 31 Jan 2024

Tyystjärvi VA, Niittynen P, Kemppinen J, et al (2023) Variability and drivers of winter near-surface temperatures over boreal and tundra landscapes. EGUsphere 2023:1–24. https://doi.org/10.5194/egusphere-2023-576

Vandewiele M, Geres L, Lotz A, et al (2023) Mapping spatial microclimate patterns in mountain forests from LiDAR. Agricultural and Forest Meteorology 341:109662. https://doi.org/10.1016/j.agrformet.2023.109662

von Arx G, Pannatier EG, Thimonier A, Rebetez M (2013) Microclimate in forests with varying leaf area index and soil moisture: Potential implications for seedling establishment in a changing climate. Journal of Ecology 101:1201–1213. https://doi.org/10.1111/1365-2745.12121

Warscher M, Wagner S, Marke T, et al (2019) A 5 km resolution regional climate simulation for Central Europe: Performance in high mountain areas and seasonal, regional and elevation-dependent variations. Atmosphere 10:682. https://doi.org/10.3390/atmos10110682

Wei T, Simko V (2021) corrplot: Visualization of a correlation matrix. R package version 0.92. https://github.com/taiyun/corrplot

Wickham H, Averick M, Bryan J, et al (2019) Welcome to the Tidyverse. Journal of Open Source Software 4:1686. https://doi.org/10.21105/joss.01686

Wilke CO (2020) cowplot: Streamlined plot theme and plot annotations for ggplot2. R package version 1.1.1. https://CRAN.R-project.org/package=cowplot

Zeileis A, Grothendieck G (2005) zoo: S3 Infrastructure for Regular and Irregular Time Series. Journal of Statistical Software 14:1–27. https://doi.org/10.18637/jss.v014.i06

Zellweger F, Coomes D, Lenoir J, et al (2019) Seasonal drivers of understorey temperature buffering in temperate deciduous forests across Europe. Global Ecology and Biogeography 28:1774–1786. https://doi.org/10.1111/geb.12991

Supplementary tables and figures

Table S2. Summary data on simulated maximum, mean, and minimum temperature offsets; macroclimate and microclimate temperature; and temperature offset predictors in Berchtesgaden National Park using the newly developed microclimate module in iLand, based on contemporary forest conditions and a year with average historical climate conditions. Summaries present mean, standard deviation (sd), and range of annual values across the entire landscape (*n* = 864,466 observations at 10 m spatial resolution).

Variable	**Units**	**Summary statistics** mean (sd) min-max
Temperature offsets		
Annual average of daily minimum microclimate temperature offset ($Tmin_{offset}$)	°C	0.81 (0.82) -1.61-2.59
Annual average of daily mean microclimate temperature offset	°C	0.05 (0.85) -2.86-2.41
Annual average of daily maximum microclimate temperature offset ($Tmax_{offset}$)	°C	-0.70 (1.11) -5.32-3.60
Macroclimate temperature		
Annual average of daily minimum macroclimate temperature ($Tmin_{macroclimate}$)	°C	3.51 (1.51) -0.83-6.43
Annual average of daily mean macroclimate temperature (mean annual temperature)	°C	5.68 (1.60) 1.24-8.97
Annual average of daily maximum macroclimate temperature ($Tmax_{macroclimate}$)	°C	7.84 (1.69) 3.31-11.51
Microclimate temperature		
Annual average of daily minimum microclimate temperature ($Tmin_{microclimate}$)	°C	4.32 (1.41) -1.07-8.00
Annual average of daily mean microclimate temperature (mean annual microclimate temperature)	°C	5.73 (1.32) 0.87-9.99
Annual average of daily maximum microclimate temperature ($Tmax_{microclimate}$)	°C	7.14 (1.41) 1.73-12.56
Other predictor variables		
Northness	dim[-1,1]	0.27 (0.64) -1-1
Topographic position index (TPI)	m	-8.95 (47.19) -105-67
Leaf area index (LAI)	m^2 m^{-2}	2.76 (2.09) 0.3-9.4
Shade tolerance (STol)	dim[1,5]	2.73 (1.02) 1-5

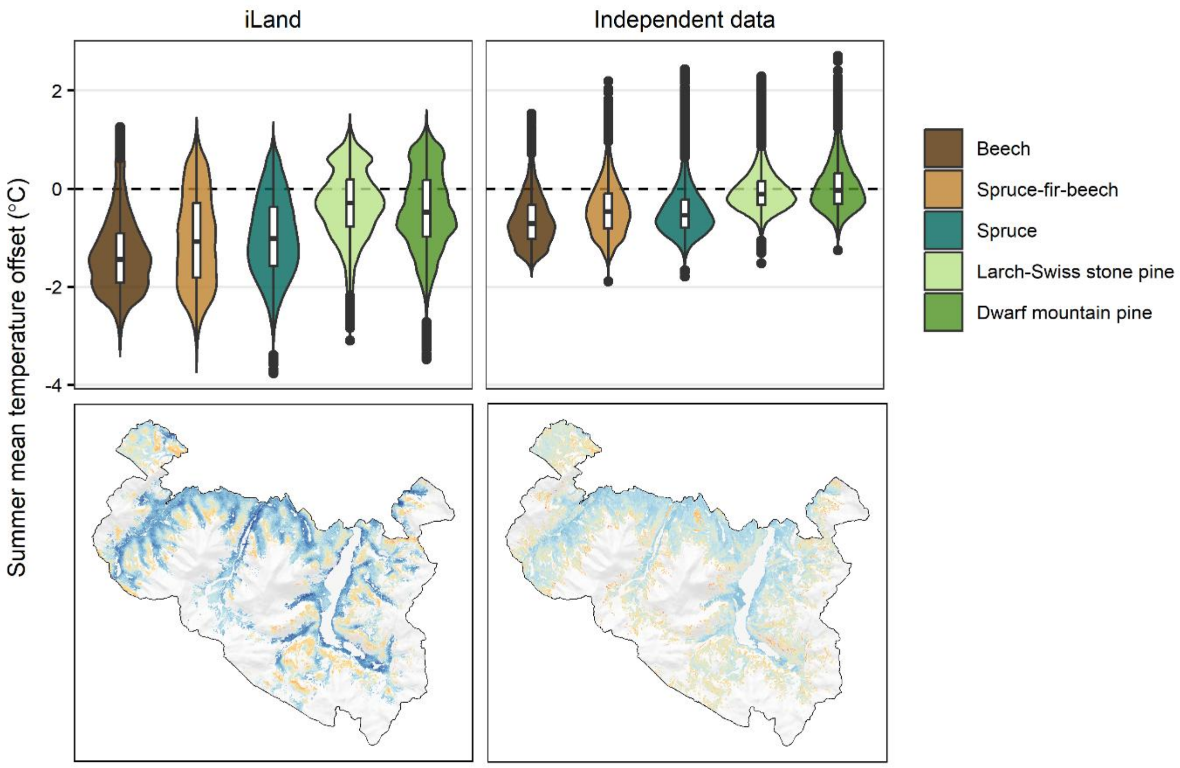

Figure S8. Comparison between simulated summer mean temperature offsets at ~1 m height in Berchtesgaden National Park using the newly developed microclimate module in iLand (left column) and temperature offset maps generated for this landscape using independent microclimate data measured at 15 cm height and mapped with LiDAR (right column; Vandewiele et al., 2023). Simulated offsets were derived at 10 m resolution (n = 864,466 observations) based on contemporary 2020 forest conditions and a year with average historical climate conditions (1988, 5.7 °C mean annual temperature). Independent data were mapped at 20 m resolution based on temperature and LiDAR data collected in 2021 (n = 229,432 observations). Corresponding values from the independent dataset were extracted using cell centroid locations from the simulated dataset, and correlation was moderately positive (Spearman's ρ = 0.47; n = 832,130 observations after removing NA values). (top row) Violin and boxplots showing summer mean minimum temperature offsets by forest type. (bottom row) Maps of summer mean temperature offsets. Mapped values are truncated to -3 and 3 to improve comparison and visualization. Temperature offsets are defined as microclimate minus macroclimate temperature.

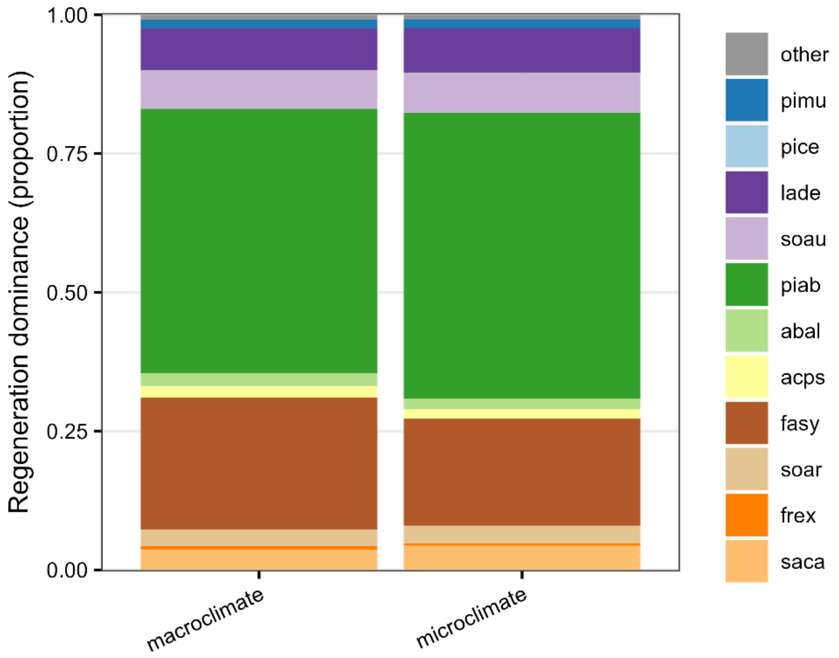

Figure S9. Tree regeneration species composition in dense forested stands (overstory LAI > 4) in microclimate versus macroclimate simulations. Stacked bars show mean proportion of total tree regeneration density for a given species across 10 simulation replicates, based on stem counts for stems < 4 m in height. Species are ordered based on whether they tend to occur at higher (pimu) to lower (saca) elevations. Species codes: pimu, *Pinus mugo*; pice, *Pinus cembra*; lade, *Larix decidua*; soau, *Sorbus aucuparia*; piab, *Picea abies*; abal, *Abies alba*; acps, *Acer pseudoplatanus*; fasy, *Fagus sylvatica*; soar, *Sorbus aria*; frex, *Fraxinus excelsior*; saca, *Salix caprea*.

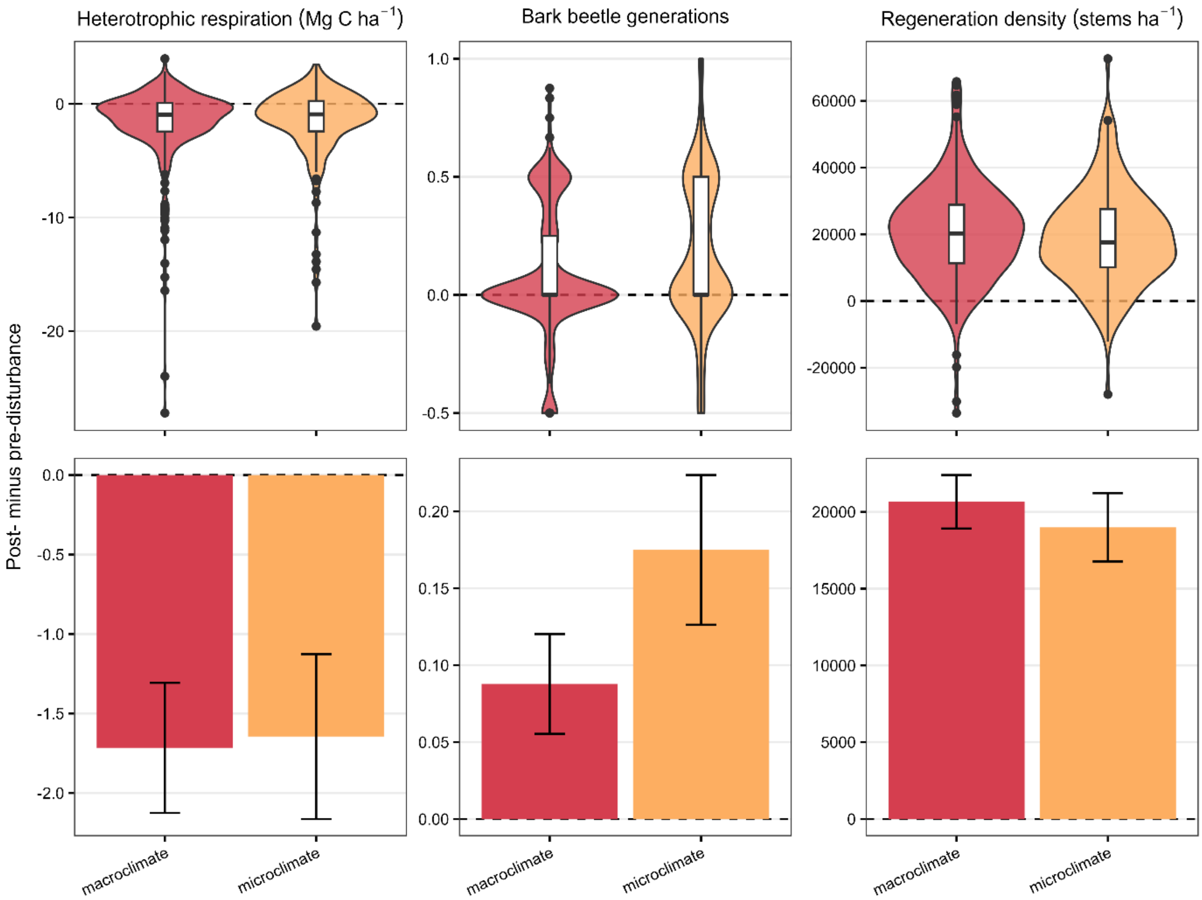

Figure S10. Disturbance effects (post- minus pre-disturbance values for each patch) on forest process indicators for microclimate and macroclimate simulations. Disturbance patches were delineated based on bark beetle and wind events occurring within the first 10 years of each simulation replicate, using the 8-neighbor rule. Pre-disturbance values were from simulation year 0, and post-disturbance values from simulation year 15 (5-15 years since disturbance). (top row) Violin and boxplots show the distribution of values across all disturbance patches (n = 283 for macroclimate, n = 165 for microclimate). (bottom row) Mean values (bars) and two standard errors (error bars) across all patches.

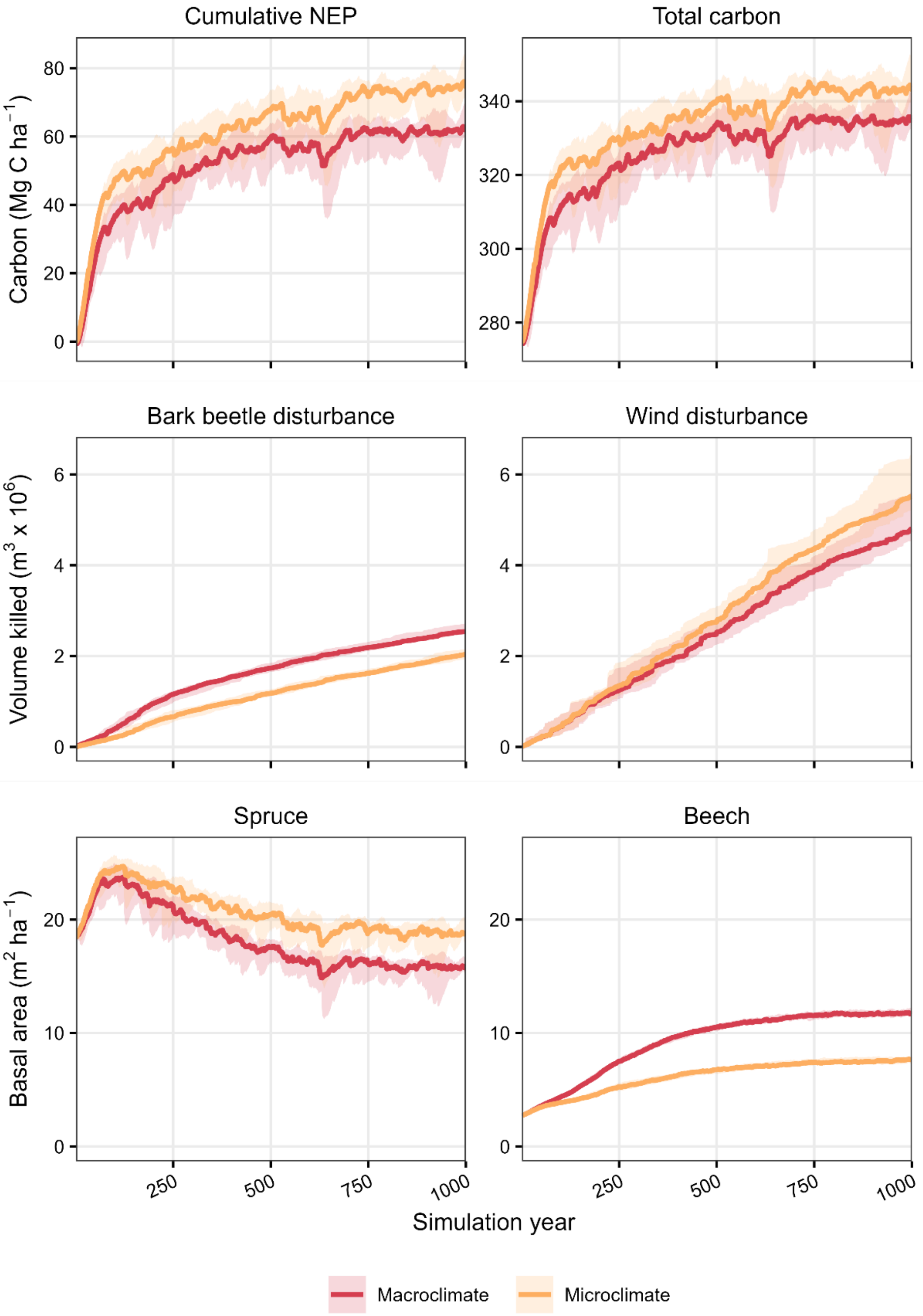

Figure S11. Landscape scale trajectories over 1,000 simulation years for cumulative net ecosystem productivity (NEP), total carbon, cumulative disturbance mortality due to bark beetles and wind, and basal area for spruce and beech, with or without microclimate temperature buffering effects. Lines are median values and shading shows 5th to 95th percentile values across 10 simulation replicates.

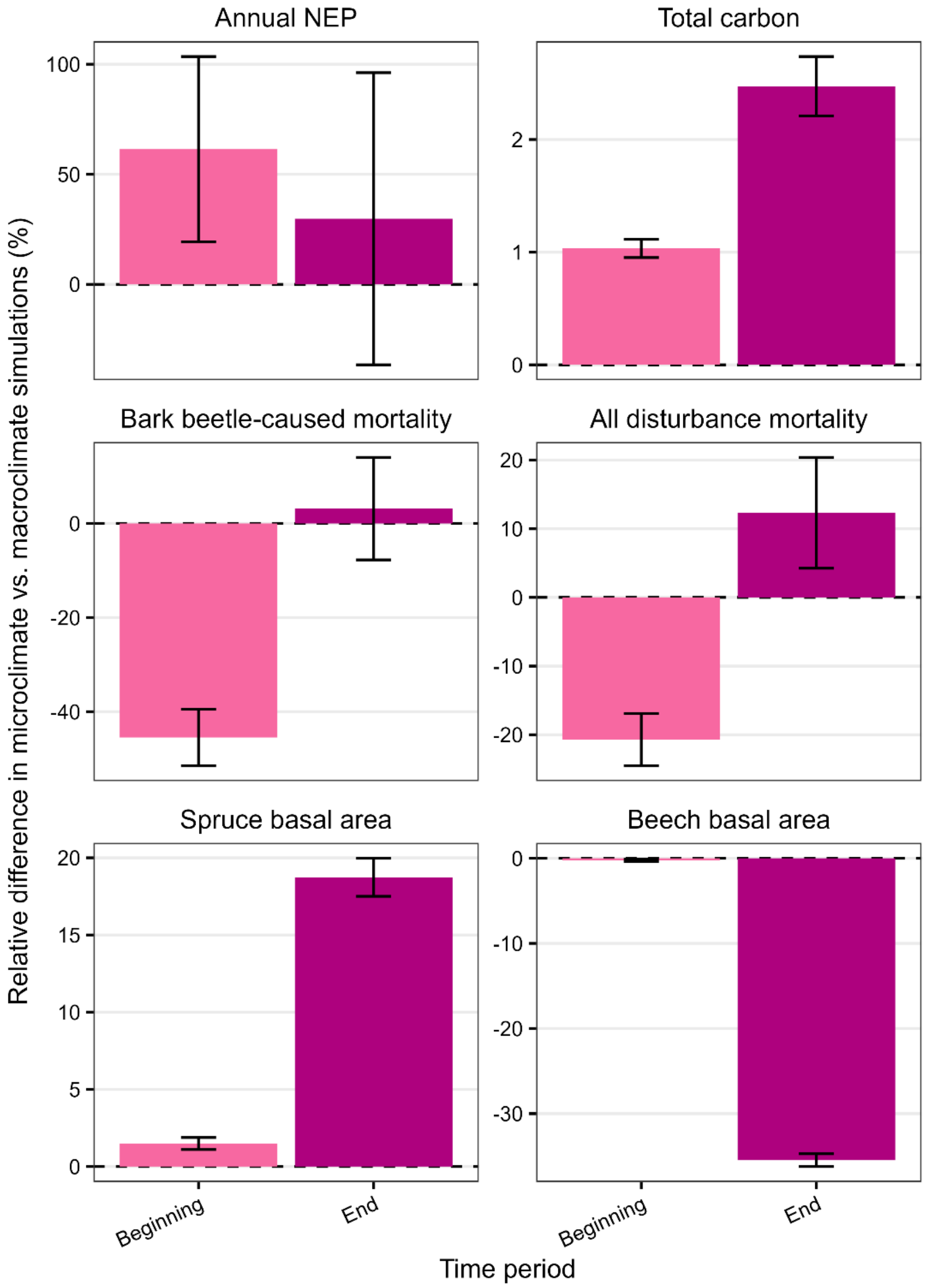

Figure S12. Change in effects of microclimate temperature buffering over time, evaluated by comparing the relative differences in landscape scale indicators at the beginning or end of 1,000 years of forest development. Annual, rather than cumulative, net ecosystem productivity (NEP), bark beetle-caused mortality, and all disturbance mortality were used to ensure comparability across different time periods. All indicators were the average of the first and last 30 simulation years. Relative values were calculated as 100 x (microclimate – macroclimate)/macroclimate. Bar height is the mean value and error bars are two standard errors (n = 10 replicates).

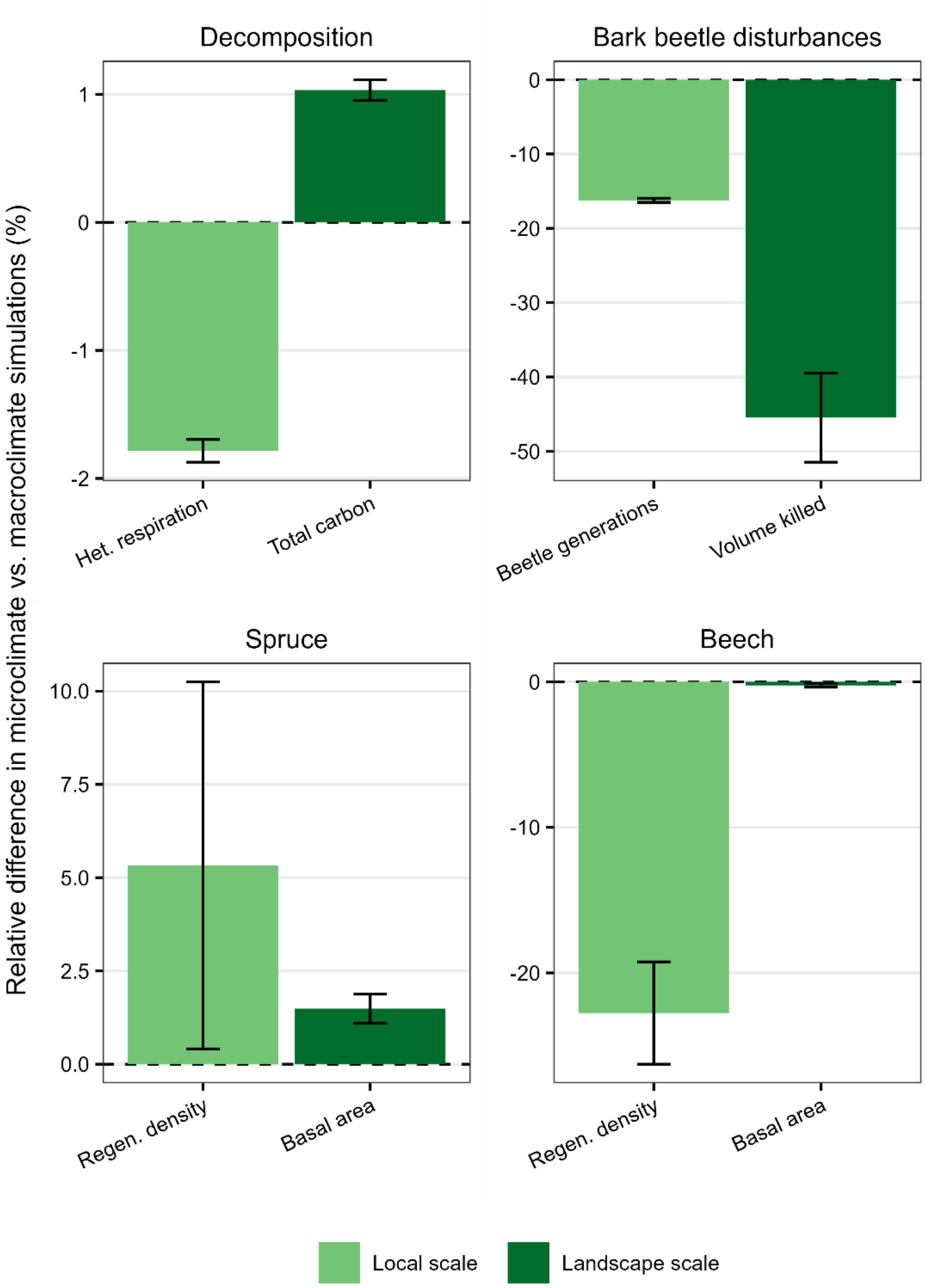

Figure S13. Change in effects of microclimate temperature buffering across scales, evaluated by comparing the relative differences in local and landscape scale indicators, with local scale indicators representing the process directly affected by microclimate temperature. All indicators were the average of the first 30 simulation years. Note that negative relative differences in respiration translate into positive relative differences in carbon (because decreased respiration leads to lower carbon losses to the atmosphere). Relative values were calculated as 100 x (microclimate – macroclimate)/macroclimate. Bar height is the mean value and error bars are two standard errors (n = 10 replicates).